Correlation functions in stable first-order relativistic hydrodynamics

Navid Abbasi,[1,*] Ali Davody,[2,†] and Sara Tahery[3,‡]

[1]*School of Nuclear Science and Technology, Lanzhou University, 222 South Tianshui Road, Lanzhou 730000, China*

[2]*SoundHound AI, Inc, 5400 Betsy Ross Drive Santa Clara, California 95054, USA*

[3]*Institute of Particle and Nuclear Physics, Henan Normal University, Xinxiang 453007, China*

(Received 2 February 2023; accepted 3 January 2024; published 5 February 2024)

First-order relativistic conformal hydrodynamics in a general (hydrodynamic) frame is characterized by a shear viscosity coefficient and two UV-regulator parameters. Within a certain range of these parameters, the equilibrium is stable and propagation is causal. In this work we study the correlation functions of fluctuations in this theory. We first compute hydrodynamic correlation functions in the linear response regime. Then we use the linear response results to explore the analytical structure of response functions beyond the linear response. A method is developed to numerically calculate the branch-cut structure from the well-known Landau equations. We apply our method to the shear channel and find the branch cuts of a certain response function, without computing the response function itself. We then solve the Landau equations analytically and find the threshold singularities of the same response function. Using these results, we achieve the leading singularity in momentum space, by which, we find the long-time tail of the correlation function. The results turn out to be in complete agreement with the loop calculations in effective field theory.

DOI: 10.1103/PhysRevD.109.036006

I. INTRODUCTION

It is well known that relativistic hydrodynamics beyond zeroth order in derivatives can be constructed in various ways, depending on how the fluid velocity and temperature are defined when the system is not in equilibrium [1]. Any particular choice of definition for these out of equilibrium variables is called a choice of "frame."[1] In the famous Eckart [2] and Landau-Lifshitz [3] frames, hydrodynamics exhibits some nonphysical features: the thermal equilibrium is unstable [4], and the theory supports the propagation of superluminal modes [5].

Problems of instability and acausality are associated with modes outside the range of validity of hydrodynamics, i.e., beyond the long wavelength low frequency limit. In other words, the problem is due to the UV modes. To remedy this, one way is to introduce extra dynamical degrees of freedom into hydrodynamics, thereby modifying the behavior of the theory in the UV. This is actually the idea of the Israel-Stewart theory [6,7]. Another way to deal with this problem is to include the second-order derivative corrections [8–10].[2] A more systematic way of dealing with this problem is to find certain out of equilibrium definitions for hydrodynamic variables, something other than those used by Eckart or Landau-Lifshitz. This program was touched on by [13,14], and built in [15,16]. These theories ([15,16]) are sometimes referred to as Bemfica-Disconzi-Noronha-Kovtun (BDNK) in the literature.[3]

In this work, we study correlation functions in BDNK theory. We first proceed to calculate the correlation functions in the linear response regime. It is discussed in Sec. III. We perform calculations separately for the sound and shear channels. The pole structure of the correlation function is found to be completely consistent with the linear excitation spectrum found in [16]. Furthermore, our calculations reveal an important feature of BDNK theory.

*abbasi@lzu.edu.cn

†adavody@soundhound.com

‡saratahery@htu.edu.cn

[1]It does not have to be confused with the concept of Lorentz frames.

Published by the American Physical Society under the terms of the Creative Commons Attribution 4.0 International license. Further distribution of this work must maintain attribution to the author(s) and the published article's title, journal citation, and DOI. Funded by SCOAP³.

[2]In practice, causal relativistic hydrodynamics can describe the evolution of hot QCD matter formed in heavy ion collisions (see [11,12] for a review).

[3]The idea of relativistic hydrodynamics in general frames [16–18] has been extended in several directions, by inclusion of charge, magnetic field, and spin [19–25], and also has been compared with other causal and stable frameworks [26–29]. See also [30], a gauge theory perspective on stable theories of hydrodynamics. See also [31,32] for more fundamental discussions about stability and causality.

We find that the special form of the BDNK equation causes the energy density correlator to develop a range of negative values. This can happen at any fixed value of momentum when we take a small frequency limit. However, this does not happen when we take the small momentum limit at a fixed frequency.

Apart from some numerical works (including [33,34]), little is known about BDNK theory in the "nonlinear" regime. The second part of this work is devoted to study the nonlinear fluctuations in BDNK theory. The main question is how the interactions between hydrodynamic modes affect the late-time behavior of the correlation functions. In conventional hydrodynamics, this question has a well-known answer. Nonlinear fluctuations lead to long-time tails with fractional powers in the real space correlation function [35,36]. This is actually due to the nonlinearity that causes branch point singularities in the correlation function [1,37,38]. In this work, we want to explore what happens to the long-time tails in BDNK theory.

In a systematic approach, this can be explored within the framework of the effective field theory of hydrodynamics. However, we choose a different route here. We use the fact that the two point correlation function of certain operators in the nonlinear regime factorize if the distribution of fluctuations is taken to be Gaussian [36]. In quantum field theory (QFT), the factorized correlation function is in the form of a Feynman integral, representing a simple loop diagram with two lines, i.e., a bubble diagram. We then follow the famous Landau method to find the singularities of the Feynman integral. Instead of computing the integral explicitly, Landau proposed a set of equations, the so-called "*Landau equations*," which are solved to specify the threshold singularities of the Feynman integral.

Keeping in mind the ideas discussed in the previous paragraph, we explore the analytic structure of the shear stress response function in Sec. IV. For some cases in effective field theory (EFT) of hydrodynamic interactions, knowing the analytic structure of the hydrodynamic response functions, including the threshold singularities as well as the branch-cut structure, is sufficient to find decay rates or cross sections without performing Feynman integration in the formal way. This is discussed at the beginning of Sec. IV B. In Sec. IV B 1, we develop a method to numerically find the location of branch cuts. To specify threshold singularities, we derive the associated Landau equations and solve them analytically in Sec. IV B 2. We show that our results are in complete agreement with recent EFT results obtained from explicit loop calculations.

Based on these results, we will calculate the long-time tail of shear stress correlation function in Sec. IV C. We find that within the validity range of BDNK theory, the long-time tail of the shear stress correlation function in BDNK theory is consistent with the long-time tail of the shear stress correlation function in conventional hydrodynamics.

Finally, in Sec. V we end with a review of the results, mentioning possible applications and discussing some follow-up directions.

Note: Throughout this paper we will refer to "Landau" in two contexts:

(1) "Landau-Lifshitz frame" (or Landau-Lifshitz hydrodynamics), which refers to some specific way of defining the fluid four-velocity beyond zeroth order in the derivative expansion.
(2) "Landau equations/conditions" refer to those equations that allow finding the singularity of the Feynman integral without explicitly performing the integration.

It should be emphasized that the above two items have nothing to do with each other.

II. FIRST-ORDER STABLE CONFORMAL HYDRODYNAMICS

In an uncharged conformal fluid, the constitutive relations in the most general frame are determined by four dimensionless numbers $\bar{p}$, $\bar{\pi}$, $\bar{\theta}$ and $\bar{\eta}$ [16]. Specializing to $D = 4$ dimensions, one writes

$$\begin{aligned} T^{\mu\nu} = {} & T^3\left(\bar{p}T + \bar{\pi}\frac{u^\lambda\partial_\lambda T}{T} + \bar{\pi}\frac{\partial_\lambda u^\lambda}{3}\right)(\eta^{\mu\nu} + 4u^\mu u^\nu) \\ & + \bar{\theta}T^3\left[\left(u^\lambda\partial_\lambda u^\mu + \frac{P^{\mu\lambda}\partial_\lambda T}{T}\right)u^\nu + (\mu \leftrightarrow \nu)\right] \\ & - \bar{\eta}T^3\sigma^{\mu\nu}. \end{aligned} \tag{2.1}$$

Note that $p = \bar{p}T^4$ is the equilibrium pressure and $\eta = \bar{\eta}T^3$ is the shear viscosity, both depending on the microscopic of the fluid. Two new transport coefficients, $\pi = \bar{\pi}T^3$ and $\theta = \bar{\theta}T^3$ are responsible for regulating the theory in the UV limit.

The stability and causality of the first-order hydrodynamics have been discussed extensively in the literature, over the past few years [15,16,18–22,24,26–29,33,34]. In the case of conformal fluid in $D = 4$ dimensions, these conditions are given by [15]

$$1 - \frac{3\bar{\eta}}{\bar{\theta}} - \frac{\bar{\eta}}{\bar{\pi}} > 0, \qquad \bar{\pi} > 4\bar{\eta}. \tag{2.2}$$

To satisfy (2.2), it is sufficient to take $\bar{\theta} > 4\bar{\eta}$ and $\bar{\pi} > 4\bar{\eta}$ [16]. These conditions ensure that in any equilibrium state specified by $u^\mu = \gamma(1, \mathbf{v}_0)$ and $T = T_0$, linearized evolution of (2.1) is always dissipative and in the light cone. Let us denote that the relativistic hydrodynamics in a general frame, i.e., (2.1), together with the conditions (2.2) is usually referred to as the "stable first-order relativistic hydrodynamics" theory.

III. CORRELATION FUNCTIONS IN THE LINEAR REGIME

As mentioned in the Introduction, the focus of this work is on correlation functions. In this section, we explore the correlation functions in the linear regime. To this end, we take $T^{\mu\nu}$ from (2.1) and linearize the hydrodynamic equations, namely $\partial_\mu T^{\mu\nu}=0$, around the equilibrium state specified by $u^\mu=\gamma(1,\mathbf{v}_0)$ and $T=$ constant. The linearized equations then govern the coupled linear evolution of $\delta\mathbf{v}$ and δT, as follows.

In conventional hydrodynamic treatments, taking $\mathbf{v}_0\neq 0$ is especially important to make the instabilities of the equilibrium manifest [4]. However, in this work, we restrict our study to the linearized equations when $\mathbf{v}_0=0$.

The conservation of energy, $\partial_\mu T^{\mu t}=0$ gives

$$\underline{\partial_t\frac{\delta T}{T}+\frac{1}{3}\boldsymbol{\nabla}\cdot\delta\mathbf{v}}+\frac{1}{12\bar{p}T}\left[\bar{\theta}\boldsymbol{\nabla}\cdot\left(\underline{\underline{\partial_t\delta\mathbf{v}+\boldsymbol{\nabla}\frac{\delta T}{T}}}\right)+3\bar{\pi}\partial_t\left(\underline{\partial_t\frac{\delta T}{T}+\frac{1}{3}\boldsymbol{\nabla}\cdot\delta\mathbf{v}}\right)\right]=0. \tag{3.1}$$

The equations of momentum conservation, $\partial_\mu T^{\mu i}=0$, give

$$\underline{\underline{\partial_t\delta\mathbf{v}+\boldsymbol{\nabla}\frac{\delta T}{T}}}+\frac{1}{4\bar{p}T}\left[\bar{\theta}\partial_t\left(\underline{\underline{\partial_t\delta\mathbf{v}+\boldsymbol{\nabla}\frac{\delta T}{T}}}\right)+\bar{\pi}\boldsymbol{\nabla}\left(\underline{\partial_t\frac{\delta T}{T}+\frac{1}{3}\boldsymbol{\nabla}\cdot\delta\mathbf{v}}\right)-\frac{4}{3}\bar{\eta}\boldsymbol{\nabla}^2\delta\mathbf{v}\right]=0. \tag{3.2}$$

The first two terms in each equation come from $T^{\mu\nu}$ of order zero, while the terms in brackets are associated with $T^{\mu\nu}$ of order 1. It is well known, and evident in the above equations, that the stable theory of hydrodynamics is constructed in such a way that the zeroth order equations emerge "with new transport coefficients $\bar{\theta}$ and $\bar{\pi}$" at the first order. If one proceeds to solve the equations perturbatively, that is, order by order in the derivative expansion, the above two coefficients will be washed out at the first order simply because the zeroth order equations are used. However, this differs from the concept of "stable relativistic hydrodynamics," where the equations must be solved nonperturbatively.

A. How to calculate correlation functions?

In the hydrodynamics literature, response functions are computed within the framework of the linear response theory [1,39]. To find a general response function such as $G_{\mathcal{R}}(t,\mathbf{k})$ we need to solve a differential equation of order 1. This is because the conventional relativistic hydrodynamic equations in an uncharged system, the Landau-Lifshitz equations, are "*parabolic*." The result can then be used to find the correlation function via the fluctuation-dissipation theorem.

However, in the "general frame" formalism [16], the hydrodynamic equations are "*hyperbolic*." Computing the response function in this case requires an extension of the standard method developed in [1,39] to second-order time-differential equations. Here we choose a different route; instead of computing the response function, we choose to compute the correlation function directly. To this end, we extend the Landau-Lifshitz method of computing the correlation function [40,41] to relativistic systems. We can then compute various correlation functions. With them, one can also use the fluctuation-dissipation theorem to find the response functions. In this work, however, our focus is on computing correlation functions. This is what we will do in the next two subsections.

B. Correlation functions in longitudinal channel

An important aspect of the "stable relativistic hydrodynamics" is that it allows us to treat fluid velocity and temperature as the hydrodynamic variables, employing the same concepts we know in thermodynamics and similar to what is done in nonrelativistic fluid dynamics. Then this suggests that in addition to the correlation functions of conserved charges (or currents), the correlation function of hydrodynamic variables, such as $\langle v_i(t_1,\mathbf{x}_1)v_j(t_2,\mathbf{x}_2)\rangle$, may also have sensible description. It should be emphasized that our main physical arguments in this paper will be made based on the correlation function of conserved densities. However, as we will explain below, each of the latter correlators is a linear combination of former ones.

Keeping in mind the above discussion, we first compute the correlation function of the hydrodynamic variables. Considering $\delta\phi_a=(\frac{\delta T}{T},\delta v_i)\equiv(\frac{\delta T}{T},\delta v^\perp,\delta v^\parallel)$, the correlation function of ϕ_a and ϕ_b is defined as

$$\langle\delta\phi_a\delta\phi_b\rangle_{\omega\mathbf{k}}=\int_{-\infty}^{+\infty}dt\int d^3\mathrm{x}e^{i\omega t}e^{-i\mathbf{k}\cdot\mathbf{x}}\times\langle\delta\phi_a(t,\mathbf{x})\delta\phi_b(0,\mathbf{0})\rangle. \tag{3.3}$$

We also find it useful to define dimensionless quantities as

$$\mathfrak{w}=\frac{\bar{\eta}}{\bar{p}}\frac{\omega}{T},\qquad \mathfrak{q}=\frac{\bar{\eta}}{\bar{p}}\frac{\mathbf{k}}{T},\qquad \pi_\eta=\frac{\bar{\pi}}{\bar{\eta}},\qquad \theta_\eta=\frac{\bar{\theta}}{\bar{\eta}}. \tag{3.4}$$

As mentioned before, we extend the method developed in [40,41] to compute various correlation function $\langle \delta\phi_a \delta\phi_b \rangle_{\mathfrak{w}\mathfrak{q}}$ relativistic systems. Details can be found in Appendix A. For example, we find that[4]

$$\begin{aligned}
\left\langle \delta v^{\parallel} \frac{\delta T}{T} \right\rangle_{\mathfrak{w}\mathfrak{q}} &= \frac{3\bar{\eta}}{4\bar{p}^2 T^4} \frac{1}{\mathcal{D}(\mathfrak{w},\mathfrak{q})} iq \Big(i\pi_\eta\ \mathfrak{w} - 4 \Big) \big(4 - i(\theta_\eta + \pi_\eta)\mathfrak{w} \big) \\
&\quad + \frac{3\bar{\eta}}{4\bar{p}^2 T^4} \frac{1}{\mathcal{D}^*(\mathfrak{w},\mathfrak{q})} (-iq) \Big(-i\theta_\eta\ \mathfrak{w} - 4 \Big) \big(4 + i(\theta_\eta + \pi_\eta)\mathfrak{w} \big), \\
\left\langle \frac{\delta T}{T} \delta v^{\parallel} \right\rangle_{\mathfrak{w}\mathfrak{q}} &= \frac{3\bar{\eta}}{4\bar{p}^2 T^4} \frac{1}{\mathcal{D}(\mathfrak{w},\mathfrak{q})} iq \Big(i\theta_\eta\ \mathfrak{w} - 4 \Big) \big(4 - i(\theta_\eta + \pi_\eta)\mathfrak{w} \big) \\
&\quad + \frac{3\bar{\eta}}{4\bar{p}^2 T^4} \frac{1}{\mathcal{D}^*(\mathfrak{w},\mathfrak{q})} (-iq) \Big(-i\pi_\eta\ \mathfrak{w} - 4 \Big) \big(4 + i(\theta_\eta + \pi_\eta)\mathfrak{w} \big) \Big].
\end{aligned} \tag{3.5}$$

As one would expect:

$$\left\langle \delta v^{\parallel} \frac{\delta T}{T} \right\rangle_{\mathfrak{w}\mathfrak{q}} = \left\langle \frac{\delta T}{T} \delta v^{\parallel} \right\rangle_{-\mathfrak{w},-\mathfrak{q}}. \tag{3.6}$$

Now let us move on to calculating the energy density correlation function, namely $G_{T_{tt}T_{tt}}(\mathfrak{w},\mathfrak{q}) = \langle T^{tt} T^{tt} \rangle_{\mathfrak{w}\mathfrak{q}}$. Using (2.1), one writes

$$\begin{aligned}
G_{T_{tt}T_{tt}}(\mathfrak{w},\mathfrak{q}) = \bar{p}^2 T^8 \Big[& 9(\pi_\eta^2 \mathfrak{w}^2 + 16) \left\langle \frac{\delta T}{T} \frac{\delta T}{T} \right\rangle_{\mathfrak{w}\mathfrak{q}} + \pi_\eta^2 q_i q_j \langle \delta v_i \delta v_j \rangle_{\mathfrak{w}\mathfrak{q}} \\
& - 3\pi_\eta q_j \left((\pi_\eta \mathfrak{w} + 4i) \left\langle \frac{\delta T}{T} \delta v_j \right\rangle_{\mathfrak{w}\mathfrak{q}} + (\pi_\eta \mathfrak{w} - 4i) \left\langle \delta v_j \frac{\delta T}{T} \right\rangle_{\mathfrak{w}\mathfrak{q}} \right) \Big].
\end{aligned} \tag{3.7}$$

Then by using the corresponding correlation functions of the hydrodynamic variables (Appendix A), we find

$$\begin{aligned}
G_{T_{tt},T_{tt}} = \frac{-6\bar{\eta} T^4 \mathfrak{q}^2}{|\mathcal{D}_L(\mathfrak{w},\mathfrak{q})|^2} \big[& +(\pi_\eta - 4)\pi_\eta^2 \theta_\eta^2 \mathfrak{q}^6 + 96(\pi_\eta^2 - 4\pi_\eta + 8)\theta_\eta \mathfrak{q}^4 + 2304(\pi_\eta - 4)\mathfrak{q}^2 \\
& + 3\mathfrak{w}^2 (-2304\pi_\eta + \pi_\eta \theta_\eta (4\theta_\eta^2 - 3(\pi_\eta - 4)\pi_\eta \theta_\eta - 8(\pi_\eta - 2)\pi_\eta) \mathfrak{q}^4 \\
& + 48(-2(\pi_\eta - 2)\pi_\eta \theta_\eta + (\pi_\eta - 4)\theta_\eta^2 + (\pi_\eta - 8)\pi_\eta^2)\mathfrak{q}^2) \\
& + 9\mathfrak{w}^4 (4\pi_\eta^3 \theta_\eta \mathfrak{q}^2 + \pi_\eta \theta_\eta^2 (\pi_\eta (3\pi_\eta - 4)\mathfrak{q}^2 - 48) - 4\pi_\eta^3 (\pi_\eta \mathfrak{q}^2 + 12)) - 27\mathfrak{w}^6 \pi_\eta^3 \theta_\eta^2 \big],
\end{aligned} \tag{3.8}$$

with

$$\mathcal{D}_L(\mathfrak{w},\mathfrak{q}) = 9\pi_\eta \theta_\eta \mathfrak{w}^4 + 36i(\theta_\eta + \pi_\eta)\mathfrak{w}^3 - 6(\pi_\eta(\theta_\eta + 2)\mathfrak{q}^2 + 24)\mathfrak{w}^2 - 12i(\theta_\eta + \pi_\eta + 4)\mathfrak{q}^2 \mathfrak{w} + ((\pi_\eta - 4)\theta_\eta \mathfrak{q}^2 + 48)\mathfrak{q}^2. \tag{3.9}$$

Solving $\mathcal{D}_L(\mathfrak{w},\mathfrak{q}) = 0$ gives the spectrum of modes associated with the longitudinal channel. This has been discussed in detail in [16]. However, we illustrate the pole structure of correlation functions associated with the sound channel in Fig. 2. As is seen, the correlation function develops a range of negative values in unstable frames. The situation shown in the figure is for $\mathfrak{q} = 1.5$. The smaller the value of $\mathfrak{q}^2$, the narrower the range of negative values around $\mathfrak{w} = 0$. Close to $\mathfrak{w} = 0$ we have

[4]Similar to (3.5), one can easily compute $\langle \frac{\delta T}{T} \frac{\delta T}{T} \rangle_{\mathfrak{w}\mathfrak{q}}$ and $\langle \delta v_z \delta v_z \rangle_{\mathfrak{w}\mathfrak{q}}$. More details can be found in Appendix A. Note that in this Appendix we take $\delta v^{\parallel} \equiv \delta v_z$.

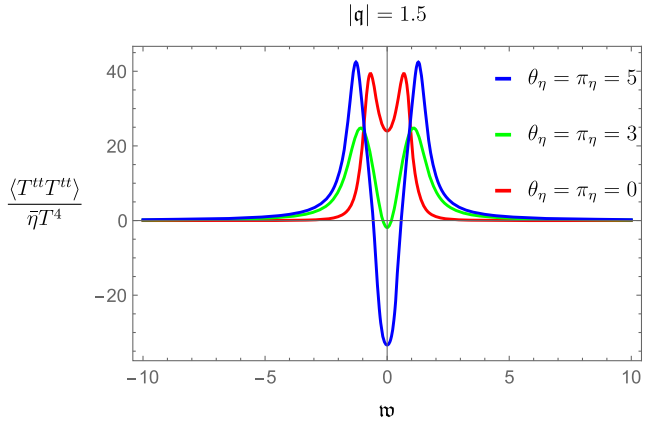

FIG. 1. Energy density correlation function in the Landau-Lifshitz frame (red), in an unstable frame (green), and in a stable frame (blue).

$$\lim_{\mathfrak{w}\to 0} G_{T_{tt}T_{tt}}(\mathfrak{w},\mathfrak{q}) = -\frac{6\bar{\eta}T^4(\pi_\eta^2\theta_\eta\mathfrak{q}^2 + 48(\pi_\eta - 4))}{\theta_\eta(\pi_\eta - 4)\mathfrak{q}^2 + 48}. \quad (3.10)$$

As is clearly seen, in a stable frame ($\theta_\eta, \pi_\eta > 4$),[5] (3.10) is negative for any value of $\mathfrak{q}^2$.[6] Of course, although $G_{T_{tt}T_{tt}}$ has such a negative value interval, it does not mean that the correlation function of a Hermitian operator can become negative, but that the relativistic hydrodynamics in the general frame has special features that lead to this result. Below, we explain what exactly these features are.

We can track this negativity by looking at (3.8). At small $\mathfrak{w}$ the first line is dominant; in a stable frame, the largest negative contribution to $G_{T_{tt}T_{tt}}$ at small $\mathfrak{q}$ then comes from the last term: $\sim(-6\bar{\eta}T^4\mathfrak{q}^2) \times 2304(\pi_\eta - 4)$. The latter itself, is coming from $\langle \frac{\delta T}{T}\frac{\delta T}{T}\rangle_{\mathfrak{w}\mathfrak{q}}$ in (3.7). This temperature correlator is calculated in Appendix A. There it is clearly seen that the expression $(\pi_\eta - 4)$ arises because the coefficient of $\mathfrak{q}^2$ in the second line of (B2) has the same factor. This is precisely because the coefficient of $\boldsymbol{\nabla}^2\delta\mathbf{v}$ in the momentum conservation equation (3.2) also has this factor.

We see that the specific form of the BDNK equations used to solve the causality and stability problems leads to the behavior observed in Fig. 1. More precisely, not imposing the first derivative on shell condition, i.e. the vanishing of the underlined expressions inside the brackets in (3.1) and (3.2), is necessary to ensure the stability of the equilibrium; however, according to the discussion in the previous paragraph, there is also another result: it will cause the energy density correlation function to be negative at the *small frequency* limit.[7] Interestingly, this feature does not appear in the *small momentum* limit when the frequency is held fixed.

Now, let us study the analytic structure of the correlation functions. This can be done by finding the roots of $\mathcal{D}_L(\mathfrak{w},\mathfrak{w}) = 0$ [see (3.9)]. The corresponding pole structure is shown in Fig. 2. As shown on the right panel of the figure, there are eight pole singularities in the complex $\mathfrak{w}$ plane at any particular value of $\mathfrak{q}$ (indicated by a specific color). Four of them located in the lower half plane correspond to retarded correlators, while four located in the upper half plane correspond to advanced correlators. The momentum range in which the BDNK spectrum is consistent with conventional relativistic hydrodynamics (shown in the left figure) is identified by the dashed circle in the right panel. We find that for $\theta_\eta = 4$ this is given by $\mathfrak{q} \lesssim 0.5$. We see that from the four modes of the BDNK spectrum in the lower half plane two of the modes lie outside this range, in agreement with [16].

C. Correlation functions in transverse channel

Among various correlation functions associated with this channel, we choose to explicitly express $G_{T_{ti_\perp}T_{ti_\perp}}(\mathfrak{w},\mathfrak{q}) = \langle T^{ti_\perp}T^{ti_\perp}\rangle_{\mathfrak{w}\mathfrak{q}}$, $i = x, y$. To this end, we first use the energy momentum tensor at linear order and write

$$G_{T_{ti_\perp}T_{tj_\perp}}(\mathfrak{w},\mathfrak{q}) = \delta_{ij}\bar{p}^2T^8\left(\theta_\eta^2\mathfrak{w}^2 + 16\right)\langle \delta v_{i_\perp}\delta v_{j_\perp}\rangle_{\mathfrak{w}\mathfrak{q}}. \quad (3.11)$$

Note that we have set the equilibrium fluid velocity to be $u^\mu = (1,0)$. Then by utilizing the correlation function of the transverse components of the velocity, found in Appendix A, we arrive at

$$G_{T_{ti_\perp},T_{tj_\perp}} = \delta_{ij}\frac{2\bar{\eta}T^4\mathfrak{q}^2}{|\mathcal{D}_T(\mathfrak{w},\mathfrak{q})|^2}(\theta_\eta^2\mathfrak{w}^2 + 16), \quad (3.12)$$

where $\mathcal{D}_T$ is the spectral function of the transverse (shear) channel:

$$\mathcal{D}_T(\mathfrak{w},\mathfrak{q}) = \theta_\eta\mathfrak{w}^2 + 4i\mathfrak{w} - \mathfrak{q}^2. \quad (3.13)$$

Solving $\mathcal{D}_T(\mathfrak{w},\mathfrak{q}) = 0$ gives the spectrum of modes associated with the transverse (shear) channel. This has been discussed in detail in [16]. However, we illustrate the pole structure of correlation functions associated with this channel in Fig. 3. In conventional hydrodynamics, there

[5]The sufficient conditions for stability and causality, discussed earlier, take a simpler form when expressed in terms of dimensionless coefficients: $\pi_\eta > 4$ and $\theta_\eta > 4$.

[6]However, for unstable frames ($\theta_\eta = \pi_\eta < 4$), this negative range may disappear depending on how small $\mathfrak{q}$ is.

[7]Note that if we impose on shell conditions on Eqs. (3.1) and (3.2), the two coefficients $\bar{\theta}$ and $\bar{\eta}$ will be washed out of the equations. Therefore, we end up with the familiar equations in the Landau-Lifshitz frame. This is equivalent to taking $\theta_\eta = \pi_\eta = 0$ in (3.10); obviously, $\lim_{\mathfrak{w}\to 0} G_{T_{tt}T_{tt}}(\mathfrak{w},\mathfrak{q}) = 24\bar{\eta}T^4$, which is a positive number.

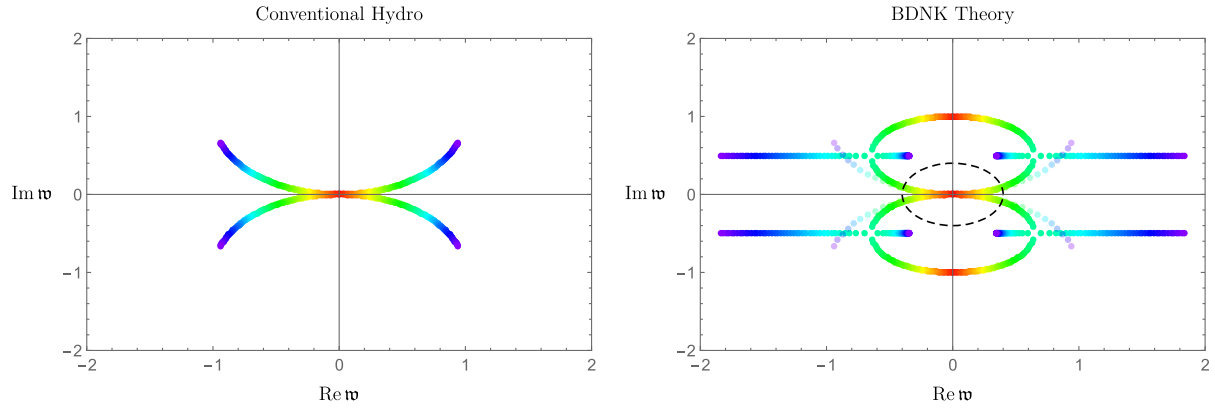

FIG. 2. Correlation functions poles comparison between conventional relativistic hydrodynamics and BDNK theory (for $\theta_\eta = \pi_\eta = 4$) in sound channel. Each colorful trajectory starting in red and ending in purple illustrates change in one single mode when q varies from 0 to 2. Lower half plane modes correspond to poles of retarded Green's functions in sound channel, while the upper half plane modes correspond to the poles of advanced Green's functions. Conventional hydro Green's functions have only two sound modes in lower half plane while BDNK theory Green's functions have two extra modes associated with the inclusion of two parameters $\bar{\theta}$ and $\bar{\pi}$. Note that to make comparison easier, we show a low-opacity version of the left panel plot on the right plot. The dashed circle shows the momentum range where the BDNK spectrum is simply consistent with the conventional relativistic hydrodynamics spectrum, i.e. $q \lesssim 0.5$ when $\theta_\eta = 4$.

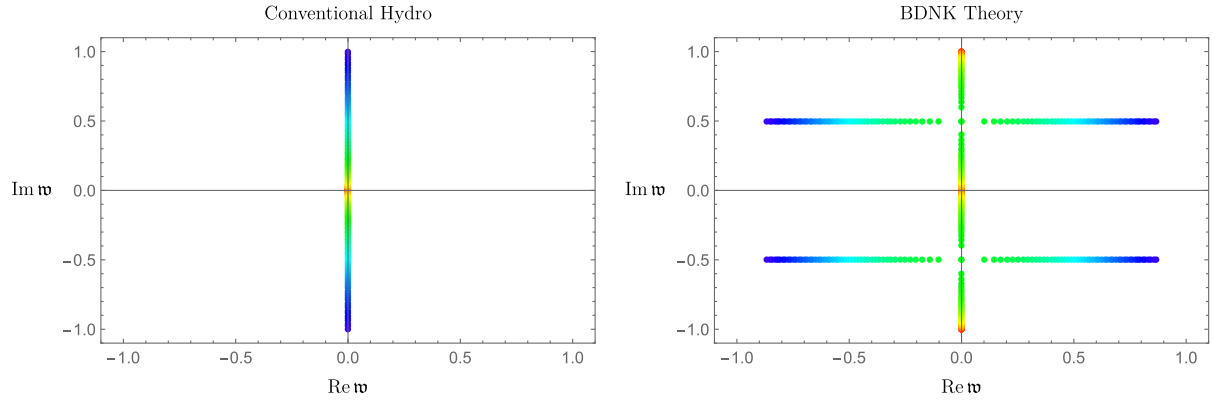

FIG. 3. Correlation functions poles comparison between conventional relativistic hydrodynamics and BDNK theory (for $\theta_\eta = 4$) in shear channel. Each colorful trajectory starting in red and ending in purple illustrates change in one single mode when q varies from 0 to 2. Lower half plane modes corresponds to poles of retarded Green's functions in shear channel, while the upper half plane modes corresponds to the poles of advanced Green's functions. Conventional hydro Green's functions have only one single shear modes in lower half plane while BDNK theory Green's functions have one more extra modes associated with the inclusion of the transport coefficient $\bar{\theta}$.

is only one shear mode above and below the complex ϖ plane, whereas in BDNK theory there is an additional mode for each half plane.[8] The latter is due to the inclusion of the UV regulator θ_η in the theory.

IV. CORRELATION FUNCTIONS BEYOND THE LINEAR REGIME

Hydrodynamics is essentially a nonlinear theory. Nonlinearities manifest as the interactions between hydrodynamic modes. A systematic approach for accounting for these interactions is to construct a hydrodynamic effective field theory [43–46]. Then from this EFT, the corrected correlation function can be found [37], showing a large renormalization of the transport coefficients [47] as well as the long-time tails [36].

These effects can also be explained by some general hydrodynamic statements [48]. Let us recall that hydrodynamic variables are macroscopically averaged values of densities over regions of size b, where $b \gg \ell_{\rm mic}$. Typically, the microscopic length scale $\ell_{\rm mic}$ is of order of the correlation length: $\ell_{\rm mic} \sim \xi$. In other words, a hydrodynamic fluctuation, such as δv, can be regarded as averaging over $(b/\xi)^3$ independent correlation volumes. According to the

[8]This is in agreement with [16].

central limit theorem, the distribution of such average will approach a Gaussian as $(b/\xi)^3 \gg 1$. The distribution is Gaussian, the non-Gaussian contribution is suppressed by an additional factor of $(b/\xi)^{-3}$, and knowledge of the two-point function at the level of the linear response is sufficient to find correlation functions beyond the linear response [36].

Following the above logic, we would like to investigate in this section the analytic structure of a certain correlation function beyond the linear response regime. This includes specifying the threshold singularity and branch-cut structure of the associated response function. We emphasize that we do not construct an effective field theory for this, but simply use the assumption that the fluctuation distribution is Gaussian.

A. Correlation function of the shear stress

To reduce technical complexity, we restrict the analysis to the correlation function of the shear stress, $G_{T_{xy}T_{xy}} = \langle T_{xy}T_{xy}\rangle$. The reason for this selection is as follows. At linear order, the shear stress T_{xy} vanishes; it just starts to contribute in quadratic order:

$$T_{xy} = 4\bar{p}T^4\delta v_x\delta v_y, \tag{4.1}$$

so the correlation function $G_{T_{xy}T_{xy}} = \langle T_{xy}T_{xy}\rangle$ is given by (n.l. stands for nonlinear)

$$G^{(\mathrm{n.l.})}_{T_{xy}T_{xy}}(t,\mathbf{x}) = w^2\langle \delta v_x(t,\mathbf{x})\delta v_y(t,\mathbf{x})\delta v_x(0,\mathbf{0})\delta v_y(0,\mathbf{0})\rangle, \tag{4.2}$$

with $w = 4\bar{p}T^4$. Since the distribution of fluctuations is assumed to be Gaussian, the above correlation can be factorized as

$$G^{(\mathrm{n.l.})}_{T_{xy}T_{xy}}(\omega,\mathbf{k}) = w^2\int\frac{d\omega'}{2\pi}\int\frac{d^3k'}{(2\pi)^3}G_{\delta v_x\delta v_x}(\omega',\mathbf{k}') \times G_{\delta v_y\delta v_y}(\omega-\omega',\mathbf{k}-\mathbf{k}'). \tag{4.3}$$

The two correlation functions in the integrand are those already calculated in the linear response regime. It is now clear why we chose to use shear stress: this is actually a special case, and to study it the only information about the linear response we need is the correlation function of velocity in the "transverse channel" (see Appendix B).

Taking $p = (\omega,\mathbf{k})$, the integrand can be written as

$$\left(\underbrace{G^{(+)}_{\delta v_x\delta v_x}(p')}_{①} + \underbrace{G^{(+)}_{\delta v_x\delta v_x}(-p')}_{②}\right) \times \left(\underbrace{G^{(+)}_{\delta v_y\delta v_y}(p-p')}_{③} + \underbrace{G^{(+)}_{\delta v_y\delta v_y}(-p+p')}_{④}\right), \tag{4.4}$$

where $(+)$ represents the one-sided Fourier transformation (see Appendix A for details). Of the four possible multiplicative terms, ① × ④ and ② × ③ do not contribute to the integral. The reason is simply that, for each of them, all pole singularities lie in only half of the complex ω' plane, either in the upper half or in the lower half. Regarding the remaining two terms, ② × ④ only contributes to the upper half plane structure of $G^{(\mathrm{n.l.})}_{T_{xy}T_{xy}}(p)$, the advanced Green's function. And finally this is the ① × ③ term which contributes to the lower half plane structure of $G^{(\mathrm{n.l.})}_{T_{xy}T_{xy}}(p)$. Therefore, to find the analytic structure of the "response function" of T_{xy}, i.e., $G^R_{T_{xy}T_{xy}}$, it is sufficient to consider the following integral:

$$\bar{w}^2\int\frac{d\omega'}{2\pi}\int\frac{d^3k'}{(2\pi)^3}G^{(+)}_{\delta v_x\delta v_x}(\omega',\mathbf{k}')G^{(+)}_{\delta v_y\delta v_y}(\omega-\omega',\mathbf{k}-\mathbf{k}') \sim \int\frac{d\mathfrak{w}'}{2\pi}\int\frac{d^3q'}{(2\pi)^3}\frac{\mathcal{N}(\mathfrak{w}')}{\mathcal{D}_T(\mathfrak{w}',\mathfrak{q}')}\frac{\mathcal{N}(\mathfrak{w}-\mathfrak{w}')}{\mathcal{D}_T(\mathfrak{w}-\mathfrak{w}',\mathfrak{q}-\mathfrak{q}')}. \tag{4.5}$$

The expression $\mathcal{D}_T$ in the denominator is the spectral function of the transverse channel that we already found in the linear response regime [see (3.13)],

$$\mathcal{D}_T(\mathfrak{w},\mathfrak{q}) = \mathbf{0}) = \theta_\eta\mathfrak{w}^2 + 4i\mathfrak{w} - \mathfrak{q}^2 = 0,$$

and it encodes the dispersion relations of the two gapped modes associated with this channel:

$$\mathfrak{w}_{1,2} = -\frac{i}{\theta_\eta}\left(2 \mp \sqrt{4-\theta_\eta\mathfrak{q}^2}\right). \tag{4.6}$$

Note that we are considering fluctuations on top of an equilibrium state with $u^\mu = (1,\mathbf{0})$.

Needless to say, the integral (4.5) is a kind of one-loop integral that we usually deal with in quantum field theory:

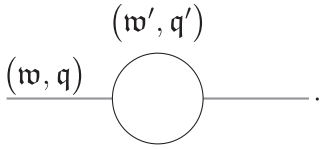

It is convenient to use Feynman parameters to rewrite (4.5) as

$$\mathcal{I}(\mathfrak{w},\mathfrak{q}) = \int \frac{d\mathfrak{w}'}{2\pi}\int \frac{d^3q'}{(2\pi)^3}\int_0^1 d\alpha_1\int_0^1 d\alpha_2\delta(\alpha_1+\alpha_2-1) \times \frac{\mathcal{N}(\mathfrak{w}')N(\mathfrak{w}-\mathfrak{w}')}{[\alpha_1\mathcal{D}_T(\mathfrak{w}',\mathfrak{q}')+\alpha_2\mathcal{D}_T(\mathfrak{w}-\mathfrak{w}',\mathfrak{q}-\mathfrak{q}')]^2}. \tag{4.7}$$

Then based on general complex analysis arguments, it is possible to discuss the analytic properties of $\mathcal{I}(\mathfrak{w},\mathfrak{q})$, without performing the frequency/momentum integral. This is basically the idea proposed by Landau in the famous paper [49]. Here, our goal is to use the Landau conditions/equations derived in [49] to find poles and branch cuts of $\mathcal{I}(\mathfrak{w},\mathfrak{q})$ in (4.7), which are actually the singularities of $G^R_{T_{xy}T_{xy}}$ as well.

B. Analytic structure of response functions from "Landau conditions/equations"

A physical question is why we should be interested in specifying the analytic structure of the response functions, while we do not have access to their explicit expressions. This can be discussed in the context of quantum field theory. In QFT, the discontinuity of the general scattering amplitude $\mathcal{M}$ can be found by using the Cutkosky algorithm [50].[9] This is done by letting all internal lines in a Feynman diagram go on shell. Knowledge of threshold singularities and branch cuts is required at this point to perform the final Feynman integration.[10] From this, Im$\mathcal{M}$ can be calculated. This might then be used to find some specific decay rate or cross section via an "optical theorem." These processes can be performed in any order in perturbation theory [50].

Our motivation for studying the analytic structure of the hydrodynamic response function is actually based on the discussion in the previous paragraph. In the context of hydrodynamics, QFT processes can be important in a variety of situations. In particular, scattering of phonon and vortex excitations is extensively discussed in the literature [51,52]. What we will do in the next two subsections is to bring some QFT methods into the context of stable first-order relativistic hydrodynamics for the first time and explore the analytic structures. These methods are not only useful in the case of BDNK theory, but also simplify loop calculations in EFT of hydrodynamics.

We first develop field-theoretic methods to specify the branch-cut structure of the shear stress response function, $G^R_{T_{xy}T_{xy}}$, in Sec. IV B 1. The threshold singularity of $G^R_{T_{xy}T_{xy}}$ can be found by applying the Landau condition to $\mathcal{I}(\mathfrak{w},\mathfrak{q})$ (see Appendix C for a brief review). This is what will be done in Sec. IV B 2. We leave the use of the results of the QFT processes to future work.

1. Branch cuts from on shell conditions

In the case of the Feynman integral (4.5) all of the kinematic dependence is encoded in the integrand. The branch cuts of such an integral are uniquely specified by where the integrand is singular on the integration contour [53]. The latter is equivalent to requiring

$$\mathcal{D}_T(\mathfrak{w}',q') = 0, \qquad \mathcal{D}_T(\mathfrak{w}-\mathfrak{w}',q\pm q') = 0. \tag{4.8}$$

These are actually on shell conditions coming from the denominator of (4.5). Note that we have used $\int\frac{d^3q'}{(2\pi)^3} = \frac{1}{(2\pi)^2}\int q'^2dq'\int_{-1}^1 d\cos\theta'$ and performed the integration over θ', which is the angle between vectors $\mathfrak{q}$ and $\mathfrak{q}'$. Let us recall that the only momentum dependence in (3.13) is a $\mathfrak{q}^2$ term. Thus $\mathcal{D}_T(\mathfrak{w}-\mathfrak{w}',q\pm q')$ depends on θ through $q^2+q'^2-2qq'\cos\theta$. Among other things, integration over θ gives a factor of

$$\ln\left(\mathcal{D}_T(\mathfrak{w}-\mathfrak{w}',q^2+q'^2-2qq'\cos\theta)\right)\Big|^{\cos\theta=1}_{\cos\theta=-1}. \tag{4.9}$$

Singularity caused by this factor is what has been given in the second equation in (4.8).

Our goal in this section is to solve the conditions (4.8). Let us assume that the entire solution is identified by the following equation:

$$s(\mathfrak{w},\mathfrak{q}) = 0. \tag{4.10}$$

For a given $\mathfrak{q}$, this equation represents a set of points in the complex $\mathfrak{w}$ plane: the set $\mathcal{S}_\mathfrak{q}$. *In the following, we introduce a method to solve (4.8), not for the function s, but directly for the set $\mathcal{S}_\mathfrak{q}$.*

Clearly, the two equations in (4.8) are the on shell conditions for the two lines of the loop when the internal momenta are parallel ($\cos\theta=\pm1$). This simply means that for a given external $(\mathfrak{w},\mathfrak{q})$, each line of the loop carries one of the two modes (4.6), in $\mathfrak{q}'||\mathfrak{q}$ conditions. We then conclude that the set $\mathcal{S}_\mathfrak{q}$ must be given by

$$\mathcal{S}_\mathfrak{q} = \bigcup_{\mathfrak{q}'||\mathfrak{q}}\bigcup_{i,j\in\{1,2\}}\{\mathfrak{w}_i(\mathfrak{q}')+\mathfrak{w}_j(\mathfrak{q}-\mathfrak{q}')\}. \tag{4.11}$$

To make things simpler, we take the external momentum directed in one specific direction: $\mathfrak{q}=(0,0,q)$. Then by reparametrizing the momenta in the loop as

[9]Note that $\mathcal{I}(\mathfrak{w},\mathfrak{q})$ above is similar to $\mathcal{M}$, although there is not any asymptotic state in the shear channel to define scattering amplitude [51].

[10]A threshold singularity is the branch point of the scattering amplitude $\mathcal{M}$. See Appendix C for more details.

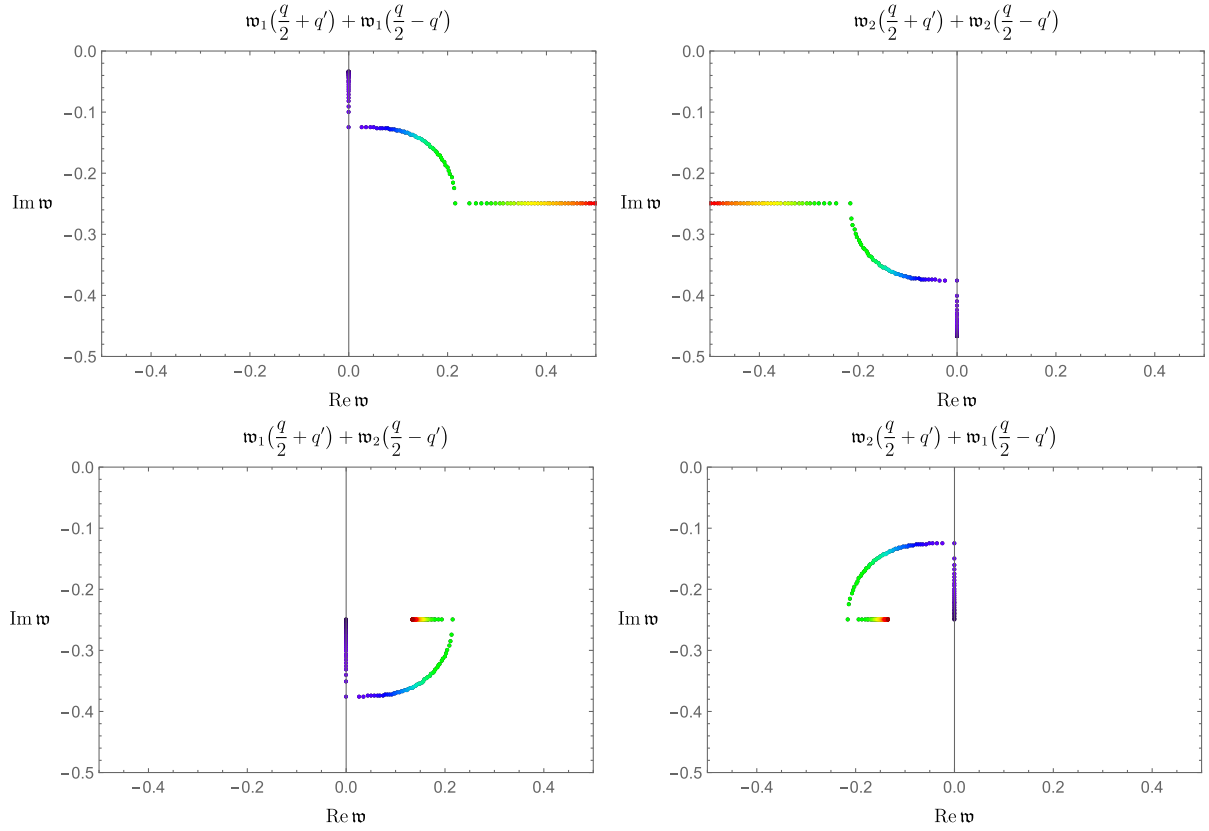

FIG. 4. Illustration of the $\mathcal{S}_{\mathfrak{q}}^{ij}$'s at $\mathfrak{q}=(0,0,q=0.5)$ in the lower half of the complex frequency plane. In each panel, we have shown values of $\mathfrak{w}_i(\frac{q}{2}+q')+\mathfrak{w}_j(\frac{q}{2}-q')$ for 150 different q' values between $0\le q'<1.5$.

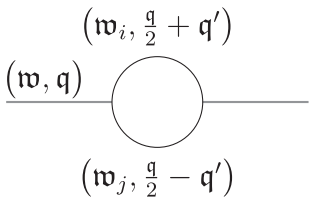

Equation (4.11) takes the following form:

$$\boxed{\mathcal{S}_{\mathfrak{q}}=\bigcup_{q'\ge 0}\bigcup_{i,j\in\{1,2\}}\left\{\mathfrak{w}_i\left(\frac{q}{2}+q'\right)+\mathfrak{w}_j\left(\frac{q}{2}-q'\right)\right\}}. \quad (4.12)$$

Regarding the evaluation of $\mathcal{S}_{\mathfrak{q}}$ above, some comments are in order:

(1) We perform the evaluation of $\mathcal{S}_{\mathfrak{q}}$ in four separate parts, $\mathcal{S}_{\mathfrak{q}}^{ij}; i,j\in\{1,2\}$, corresponding to the various values the pair (i,j) may take.
(2) At a given q, for each part, e.g., $(i,j)=(1,1)$, we calculate $\mathfrak{w}_i(\frac{q}{2}+q')+\mathfrak{w}_j(\frac{q}{2}-q')$ in a large number of non-negative values of q'.
(3) It turns out that for a particular (i,j), the points $\mathfrak{w}_i(\frac{q}{2}+q')+\mathfrak{w}_j(\frac{q}{2}-q')$ form a curve with two cusp points in the complex $\mathfrak{w}$ plane.
(4) Depending on (i,j), the points corresponding to $\mathfrak{w}_i(\frac{q}{2}+q')+\mathfrak{w}_j(\frac{q}{2}-q')$ are accumulated around those associated with either $q'=0$ or $q'\to\infty$.

As we will see below, the last two comments above point to the branch-cut and branch point singularities of $\mathcal{I}$ (or equivalently $G^R_{T_{xy}T_{xy}}$), respectively.

Specializing to $\theta_\eta=16$ in (4.6), we have shown the four parts of $S_{\mathfrak{q}}$, for $\mathfrak{q}=0.5$, in Fig. 4. In each panel, the four comments below (4.12) can be clearly seen. Each colored trajectory starts in purple at $q'=0$ and ends in dark red at $q'=1.5$. We have checked that by taking large values of q', no significant features are added to these plots.

The set of the four parts of $\mathcal{S}_{\mathfrak{q}}$ depicted in Fig. 4 have been shown in the top left panel of Fig. 5. This figure actually shows the entire branch-cut structure of $G^R_{T_{xy}T_{xy}}$, as the complete solution to (4.8). As it is seen, four branch points have been induced: $\mathfrak{w}_{ij}$: $i,j=1,2$. Each of these points actually corresponds to producing a pair of on shell excitations $\mathfrak{w}=\mathfrak{w}_i(\mathfrak{q})$ and $\mathfrak{w}=\mathfrak{w}_j(\mathfrak{q})$, in the loop. We show the latter in the next subsection by solving the Landau loop equations analytically.

In the same regard, more recently, Ref. [42] announced some analytical results on the structure of branch cuts in the

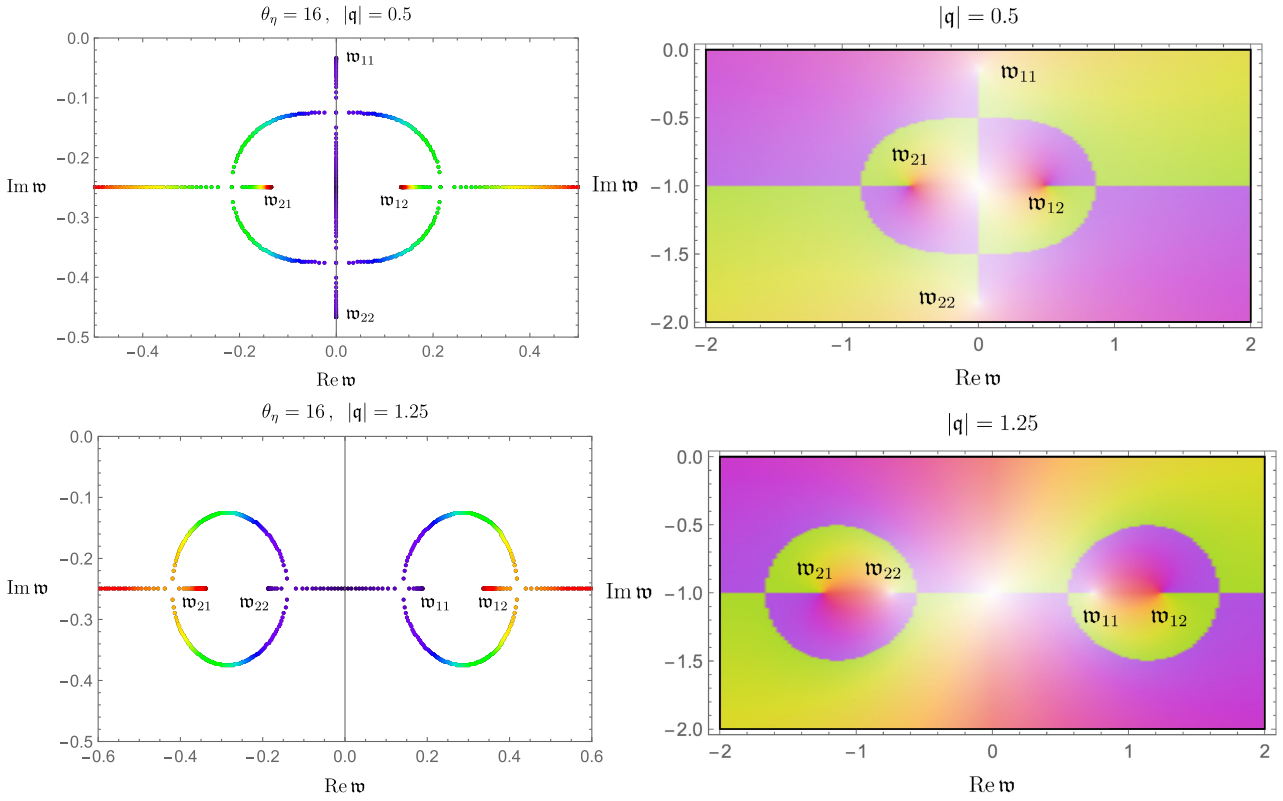

FIG. 5. Left panel: branch-cut structure of $G^R_{T_{xy}T_{xy}}$, found from solving the on shell equations. Four branch point singularities $\mathfrak{w}_{11}$, $\mathfrak{w}_{22}$, $\mathfrak{w}_{12}$, and $\mathfrak{w}_{12}$ correspond to the four parts of $\mathcal{S}_\mathfrak{q}$, shown in Fig. 4. Right panel: branch-cut structure of G^R_{nn}, found from explicit loop calculations. The right panel plots are taken from [42].

theory of "UV-regulated nonlinear diffusion." The on shell condition in this theory is given by

$$\tau^2\omega^2 + i\tau\omega - \mathfrak{q}^2 = 0, \tag{4.13}$$

where τ is the relaxation time. A comparison between this equation and the on shell condition in our present case, namely (3.13), shows that the two cases will be the same if one takes

$$\boxed{\theta_\eta = 16 \text{ in this paper}} \quad \text{vs} \quad \boxed{\tau = 4}. \tag{4.14}$$

The (top) left panel of Fig. 5 has been already produced for the value of θ_η mentioned in (4.14). In the (top) right panel of Fig. 5, we have shown the branch-cut structure of the response function in Ref. [42], at $\tau = 4$, and for the same value of $\mathfrak{q}$ taken in the left panel. Note that this reference shows the result in dimensionless frequency $\mathfrak{w} = \tau\omega$. Therefore, for comparing it with the left panel, all numbers on both of its axes must be divided by 4. Doing so, *we find that the two panels are in perfect agreement with each other.*

By increasing the value of $\mathfrak{q}$, $\mathfrak{w}_{11}$ and $\mathfrak{w}_{22}$ move closer to each other and collide at $\mathfrak{q} = 1$. As the second case to illustrate, we have considered $\mathfrak{q} = 1.25$. Repeating the procedure used at $\mathfrak{q} = 0.5$, we solve Eq. (4.8) numerically, by use of (4.12). The four $\mathcal{S}^{ij}_\mathfrak{q}$ are shown in Fig. 6. The entire branch-cut structure and threshold singularities are given in the bottom left panel of Fig. 5. Again, we see that the results are exactly in line with the most recent results of Ref. [42] in the theory of UV-regulated nonlinear diffusion, shown in the bottom right panel.

Let us emphasize that the left and right panels of Fig. 5 have been found through two different methods; the left figures were obtained by developing a new numerical method to solve the on shell equations. However, the right panel results are the result of explicit loop calculations in Ref. [42]. The branch-cut structure shown in the left panel of Fig. 5 is the central result of this section.

2. Solving Landau equations

The on shell conditions (4.8) identify where singularities can occur in the integrand. However, it is not sufficient for these singularities to develop in the full integral because we can deform the integral contour in a way that avoids these singularities. The singularity of the integrand will be the singularity of the integral, i.e., a branch point, if it cannot be avoided by doing any contour deformation. One way to

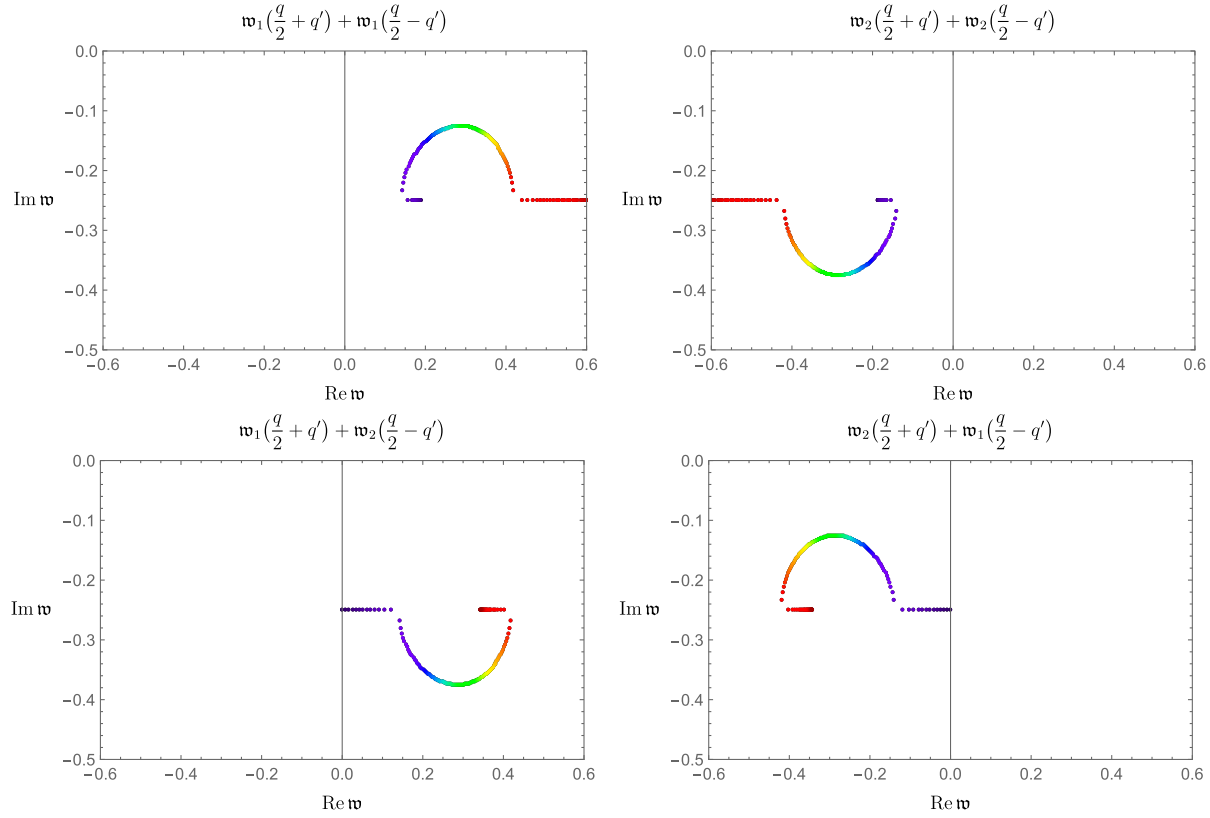

FIG. 6. Illustration of the $\mathcal{S}^{ij}_{\mathfrak{q}}$'s at $\mathfrak{q}=(0,0,q=1.25)$ in the lower half of the complex frequency plane. In each panel, we have shown values of $\mathfrak{w}_i(\frac{q}{2}+q')+\mathfrak{w}_j(\frac{q}{2}-q')$ for 150 different q' values between $0\le q'<1.5$.

obtain these points is to have the integration contour be pinched between the singularities of the integrand. Such points are called "pinch singularities" (see the Appendix C 1 for details).

Landau developed a method of finding pinched singularities (among other singularities) of the integrand in perturbation quantum field theory [49]. To briefly see how, let us rewrite the denominator of the integrand in (4.7) as

$$f^2\equiv\left[\alpha_1\mathcal{D}(\mathfrak{w}',\mathfrak{q}')+\alpha_2\mathcal{D}(\mathfrak{w}-\mathfrak{w}',\mathfrak{q}-\mathfrak{q}')\right]^2. \tag{4.15}$$

We can always make a transformation in the variables $\mathfrak{w}'$ and $\mathfrak{q}'$ to eliminate the terms linear with respect to the integral variables: $\mathfrak{w}'\equiv\mathfrak{w}'(\mathfrak{w}'')$ and $\mathfrak{q}'\equiv\mathfrak{q}'(\mathfrak{q}'')$ where $\mathfrak{w}'$ (and $\mathfrak{q}'$) differs from $\mathfrak{w}''$ (and $\mathfrak{q}''$) by a constant. It is easy to find the explicit form of the transformation; however, we only need the final form of f:

$$f=\varphi(\mathfrak{w},\mathfrak{q};\alpha_i)+K(\mathfrak{w}''^2,\mathfrak{q}''^2;\alpha_i), \tag{4.16}$$

where

$$\varphi(\mathfrak{w},\mathfrak{q};\alpha_i)=\frac{4(\alpha_1^2+\alpha_2^2)}{\theta_\eta(\alpha_1+\alpha_2)}+\frac{\alpha_1\alpha_2}{\theta_\eta(\alpha_1+\alpha_2)}\times\left(\theta_\eta^2\mathfrak{w}^2+8i\theta_\eta\mathfrak{w}-\theta_\eta\mathfrak{q}^2-8\right) \tag{4.17}$$

$$K(\mathfrak{w}''^2,\mathfrak{q}''^2)=(\alpha_1+\alpha_2)\left(\theta_\eta\mathfrak{w}''^2-\mathfrak{q}''^2\right). \tag{4.18}$$

We can make another change of variable $q''\to i\tilde{\mathfrak{q}}''$ to make K positive definite:

$$K\left(\mathfrak{w}''^2,\mathfrak{q}''^2;;\alpha_i\right)=(\alpha_1+\alpha_2)\tau\mathfrak{w}''^2+\tilde{\mathfrak{q}}''^2. \tag{4.19}$$

Now if $\varphi>0$ for all values of α_i, performing $\mathfrak{w}''$- and $\tilde{\mathfrak{q}}''$-integration does not develop any singularity. On the other hand if for some values of α_i we have $\varphi<0$, the integral becomes complex. In this case, for a given momentum $\mathfrak{q}$, the nearest singularity of integral corresponds to values of $\mathfrak{w}(\mathfrak{q})$ where φ vanishes for some particular values of α_i and is positive at all other values of α_i. In other words by treating φ as being a function of α_i, the singularities correspond to the vanishing of $\varphi(\alpha_i)$ at its minimum point[11]:

$$\varphi(\alpha_i)=0,\qquad\frac{\partial\varphi(\alpha_i)}{\partial\alpha_i}=0. \tag{4.20}$$

To simplify the second condition above, let us denote that from (4.16) it is clear that

[11]If the singularities in the complex region are meant, any extremum of function φ should be considered [49].

$$\varphi(\alpha_i) = f\Big|_{\frac{\partial f}{\partial \mathfrak{w}''}=0,\frac{\partial f}{\partial \mathfrak{q}''}=0}. \tag{4.21}$$

Since $\mathfrak{w}'$ (and $\mathfrak{q}'$) differs from $\mathfrak{w}''$ (and $\mathfrak{q}''$) by a constant, the two conditions in (4.21) can also be written as

$$\boxed{\frac{\partial f}{\partial \mathfrak{w}'} = 0, \qquad \frac{\partial f}{\partial \mathfrak{q}'} = 0}. \tag{4.22}$$

Therefore $\varphi(\alpha_i)$ is the same as f when the above additional conditions are imposed. Thus instead of differentiating φ in the second equation in (4.20), we can differentiate f with respect to α_i and then impose the two conditions above. We arrive at

$$\frac{\partial \varphi(\alpha_i)}{\partial \alpha_i} = \frac{\partial f}{\partial \alpha_i} = 0. \tag{4.23}$$

Applying this to (4.15), we get the two on shell conditions

$$\boxed{\mathcal{D}(\mathfrak{w}', \mathfrak{q}') = 0, \qquad \mathcal{D}(\mathfrak{w} - \mathfrak{w}', \mathfrak{q} - \mathfrak{q}') = 0}. \tag{4.24}$$

Equations (4.22) and (4.24) are the Landau conditions/equations for the BDNK theory, at 1-loop order. Equation (4.22) are also called "*Landau loop equations*." In the Appendix C 1, we review the original equations derived by Landau for the scalar field theory. Compared to the on shell condition in the original derivation of Landau [see (C3)], here our on shell condition is not a covariant equation [see (3.13)].

Before solving the Landau equation, let us express that any point $(\mathfrak{w}, \mathfrak{q})$ satisfying (4.22) and (4.24) is indeed a pinched singularity of the integrand. We need to remember that when two curves are tangent, their normal vectors at the point of intersection are parallel. In other words, a linear combination of normal vectors vanishes. The Eq. (4.22) are very similar to this case; they can be written as

$$\begin{aligned} \alpha_1 \frac{\partial \mathcal{D}(\mathfrak{w}', \mathfrak{q}')}{\partial \mathfrak{w}'} + \alpha_2 \frac{\partial \mathcal{D}(\mathfrak{w} - \mathfrak{w}', \mathfrak{q} - \mathfrak{q}')}{\partial \mathfrak{w}'} = 0 \\ \alpha_1 \frac{\partial \mathcal{D}(\mathfrak{w}', \mathfrak{q}')}{\partial \mathfrak{q}'} + \alpha_2 \frac{\partial \mathcal{D}(\mathfrak{w} - \mathfrak{w}', \mathfrak{q} - \mathfrak{q}')}{\partial \mathfrak{q}'} = 0. \end{aligned} \tag{4.25}$$

We see that the gradient of on shell conditions (with respect to loop momentum and frequency) is linearly dependent. This shows that solving (4.24) and (4.25) is equivalent to finding pinch singularities of the integrand on the integration contour.

Let us now proceed to solve the Landau loop equations:

$$\begin{aligned} \frac{\partial f}{\partial \mathfrak{w}'} = 0 \to \mathfrak{w}' &= \frac{\alpha_2}{\alpha_1 + \alpha_2}\mathfrak{w} + \frac{\alpha_2 - \alpha_1}{\alpha_2 + \alpha_1}\frac{2i}{\theta_\eta}, \\ \frac{\partial f}{\partial \mathfrak{q}'} = 0 \to \mathfrak{q}' &= \frac{\alpha_2}{\alpha_1 + \alpha_2}\mathfrak{q}. \end{aligned} \tag{4.26}$$

Substituting the above two expressions into the on shell conditions, we arrive at

$$\frac{\partial f}{\partial \alpha_1} = 0 \to 0 = 4 - \frac{\alpha_1^2}{(\alpha_1 + \alpha_2)^2}\left(\theta_\eta \mathfrak{q}^2 + (4 - i\theta_\eta \mathfrak{w})^2\right), \tag{4.27a}$$

$$\frac{\partial f}{\partial \alpha_2} = 0 \to 0 = 4 - \frac{\alpha_2^2}{(\alpha_1 + \alpha_2)^2}\left(\theta_\eta \mathfrak{q}^2 + (4 - i\theta_\eta \mathfrak{w})^2\right). \tag{4.27b}$$

Now we perform the integration over α_2, which replaces α_2 with $1 - \alpha_1$. We also omit the subscript of α_1. From (4.27a), we find the solution for α, i.e., α^*, as

$$\alpha^* = \frac{2}{\sqrt{\theta_\eta \mathfrak{q}^2 + (4 - i\theta_\eta \mathfrak{w})^2}}. \tag{4.28}$$

According to Ref. [49], the above α^* may be associated with the threshold singularity of the response function. Substituting this value into the second on shell condition (4.27b), we arrive at

$$-16 - \theta_\eta \mathfrak{q}^2 + 8i\theta_\eta \mathfrak{w} + \theta_\eta^2 \mathfrak{w}^2 + 4\sqrt{\theta_\eta \mathfrak{q}^2 + (4 - i\theta_\eta \mathfrak{w})^2} = 0. \tag{4.29}$$

This equation[12] has four roots:

$$\mathfrak{w} = -\frac{i}{\theta_\eta}\left(4 \pm \sqrt{16 - \theta_\eta \mathfrak{q}^2}\right), \tag{4.30a}$$

$$\mathfrak{w} = -\frac{4i}{\theta_\eta} \pm |\mathfrak{q}|\sqrt{\frac{1}{\theta_\eta}}. \tag{4.30b}$$

It is easy to check that the two roots identified by (4.30a) correspond to the threshold singularities $\mathfrak{w}_{11}$ and $\mathfrak{w}_{22}$ in Fig. 5, while the roots given by (4.30b) correspond to $\mathfrak{w}_{12}$ and $\mathfrak{w}_{21}$ in the same figure. Note that the $\mathfrak{w}_{ij}$'s shown in Fig. 5 were all found numerically; now, here we see that they can be expressed by two explicit analytic formulas (4.30a) and (4.30b).

[12]This kind of equation that constrains the external momenta and frequencies to obey the Landau equations is called the "Landau curve" [54].

Let us now evaluate (4.28) at (4.30a) and (4.30b). One finds

$$\alpha_1 = \alpha_2 \equiv \alpha^*\big|_{\text{at (4.30a)}} = \frac{1}{2} \tag{4.31a}$$

$$\alpha_1 = 1 - \alpha_2 \equiv \alpha^*\big|_{\text{at (4.30b)}} \to +\infty. \tag{4.31b}$$

This simply tells us that $\mathfrak{w}_{11}$ and $\mathfrak{w}_{22}$ are normal thresholds, i.e., $0 < \alpha^* < 1$ [53], while $\mathfrak{w}_{12}$ and $\mathfrak{w}_{21}$ are second-type singularities, because α^* is infinite [54] (see Appendix C for more details on these two types of singularities).

Let us summarize. We first numerically specified the branch-cut structure of the shear stress response function, based on the formula (4.12). The results are given in the left panel of Fig. 5. Then to find the threshold singularities shown in the figure, i.e., $\mathfrak{w}_{i,j}:\ i,j\in\{1,2\}$, we analytically solved the well-known Landau equations. *The four threshold singularities found in* (4.30a) *and* (4.30b), *and the branch-cut structure of* Fig. 5 *are exactly consistent with the results of the loop calculations in* Ref. [42].

As discussed at the beginning of Sec. IV B, knowledge of the analytic structure is useful for discovering discontinuities in scattering amplitudes in field theory. The latter can then be used to find some specific decay rates or cross sections. These field theory quantities are also calculated in EFT of hydrodynamics [51,52]. However, to the best of our knowledge, so far, no work has used the analytic structure discussed in our paper to find such quantities in the context of hydrodynamics. Our work is actually a first step in this direction. We leave the explicit field theory calculations to future work.

C. Long-time tails

In previous sections we elaborated on the analytic structure of $G^R_{T_{xy}T_{xy}}(\omega,\mathbf{k})$. The result is simple. In the linear regime it is analytic in the entire lower half complex ω plane except for the location of two simple poles (4.6). However, we showed that nonlinear effects significantly affect this behavior. For example in the small $\mathfrak{q}^2 \propto \mathbf{k}^2$ limit, $G^R_{T_{xy}T_{xy}}(\omega,\mathbf{k})$ found the complicated analytic structure illustrated in the top panel of Fig. 5.

Our main goal in this section is to investigate the effect of nonlinearities, in particular the analytic structure shown in Fig. 5, on the late-time behavior of $G^R_{T_{xy}T_{xy}}(t,\mathbf{k})$ defined as the following:

$$G^R_{T_{xy}T_{xy}}(t,\mathbf{k}) = \int \frac{d\omega}{2\pi} G^R_{T_{xy}T_{xy}}(\omega,\mathbf{k}) e^{-i\omega t}. \tag{4.32}$$

We aim to do this without explicitly evaluating the above Fourier integral. The reason is simply that we do not access the closed form of $G^R_{T_{xy}T_{xy}}(\omega,\mathbf{k})$; we only have some information about its analytic properties. However we will show that this information is sufficient to find the behavior of $G^R_{T_{xy}T_{xy}}(t,\mathbf{k})$ at late times.

To proceed, let us mention a few comments which will guide us to track the path.

(1) Nonlinear effects cause long-time tails in correlation functions. This behavior is directly related to the presence of singularities in the momentum space correlation functions [36].
(2) In BDNK theory, the shear stress correlation function has four branch point singularities (see top panel of Fig. 5). One would expect at late times, i.e., times larger than any specific timescale of the theory, the branch point $\mathfrak{w}_{11}$ to give the dominant contribution. It can be simply understood by looking at $e^{-i\omega t}$ in the integrand; this factor is exponentially decaying in the vicinity of each of the branch points. Clearly, the decay associated with $\mathfrak{w}_{12}$, $\mathfrak{w}_{21}$ and $\mathfrak{w}_{22}$ is much faster than that of $\mathfrak{w}_{11}$. This justifies why at late times, we only need to consider the *leading order* singularity at $\mathfrak{w}_{11}$.
(3) *How to find the leading order singularity around a branch point*? This question has also been answered by Landau in [49] (see the next subsection).

Thus, what we are going to do is to first introduce Landau's method of finding leading singularity of the integral in the vicinity of a branch point. Then we will apply it to $G^R_{T_{xy}T_{xy}}(\omega,\mathbf{k})$ of the BDNK theory near the branch point $\mathfrak{w}_{11}$. Finally, we will evaluate (4.32) to find the long-time tail.

1. Nature of singularities

Let us assume that the extremum value of $\varphi(\mathfrak{w},\mathfrak{q};\alpha_i)$ in (4.16) is $\varphi(\mathfrak{w},\mathfrak{q};\alpha^*)$. It was shown by Landau that the leading singularity of the integral is then given by [49]

$$\sim \text{constant}\cdot(\varphi(\mathfrak{w},\mathfrak{q};\alpha^*))^{\frac{1}{2}m-n}, \tag{4.33}$$

where m is the number of independent integrations and n is the number of internal lines in the corresponding Feynman integral. In Appendix C 2, we have evaluated m in d-dimension in terms of n and V (V is the number vertices in the diagram). For the simple bubble diagram corresponding to (4.7), clearly $n = 2$ and $m = 4 + 1$. In the latter, 4 refers to integration over $\mathfrak{w}$ and $\mathfrak{q}$, while 1 corresponds to integration over one single independent α. As a result, near the threshold specified by the solution of Landau equations, the integral corresponding to the bubble diagram behaves as[13]

$$G^R_{T_{xy}T_{xy}}(\mathfrak{w},\mathfrak{q}) \equiv \mathcal{I}(\mathfrak{w},\mathfrak{q}) \sim \text{constant}\cdot\left(\varphi(\mathfrak{w},\mathfrak{q};\alpha^*)\right)^{\frac{1}{2}}. \tag{4.34}$$

[13]The constant in front of (4.34) can be found by using the discussion given in the end of Section 1.5 in [55].

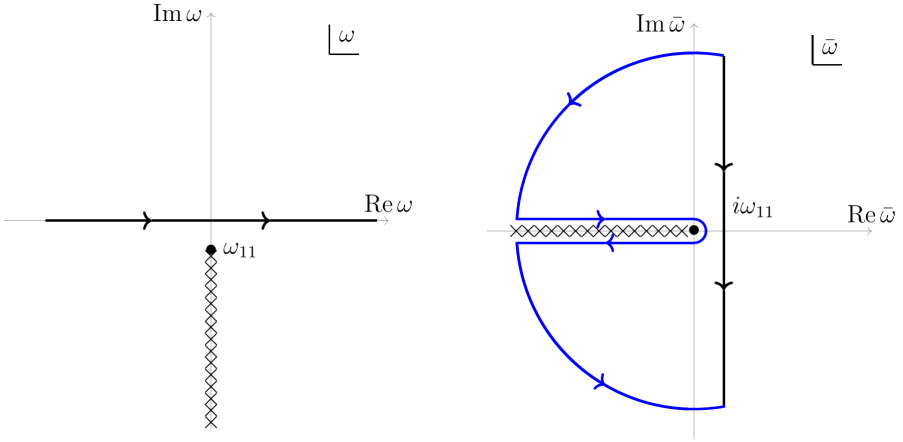

FIG. 7. Left panel: the dominant part of the analytic structure of $G^R(\omega,\mathbf{k})$ at late times. Right panel: changing the integral variable from ω to $\bar{\omega}$ and contour deformation. Note that $i\omega_{11}=(1-\sqrt{1-\theta\eta\frac{\mathbf{k}^2}{w^2}})\frac{w}{\theta}$ is real valued.

In next subsection we will evaluate this expression in BDNK theory and then use the result to find the long-time tail behavior of the $G^R_{T_{xy}T_{xy}}(t,\mathbf{k})$.

2. Long-time tails in BDNK theory

The expression of $\varphi(\mathfrak{w},\mathfrak{q};\alpha)$ for the shear stress in BDNK theory was already found in (4.17). However, as discussed before, $\mathcal{I}(\mathfrak{w},\mathfrak{q})$ has four branch point singularities $\mathfrak{w}_{ij}$: $i,j\in\{1,2\}$. The value of α^* corresponding to $\mathfrak{w}_{11}$ is $1/2$ [see (4.31a) and (4.31b)]. Using the latter, we find

$$\varphi(\omega,\mathbf{k};\alpha^*=1/2)=\omega+i\frac{\eta}{2w}\mathbf{k}^2-i\frac{\theta}{2w}\omega^2. \tag{4.35}$$

Note that we have used (3.4) to return all quantities to their dimensionful versions ($w=4p$). From now on, we will represent the results in terms of dimensionful quantities.

Let us emphasize that $\alpha^*=1/2$ corresponds to ω_{22} as well. In other words, setting $\varphi(\omega,\mathbf{k};\alpha^*=1/2)=0$ in (4.35) gives the two branch points ω_{11} and ω_{22}. But we only need to find the leading singularity near ω_{11}. For this reason, we change the variable as $\omega=\omega_{11}+i\bar{\omega}$, and expand $\varphi(\omega,\mathbf{k};\alpha^*=1/2)$ about $\bar{\omega}=0$ to the first nonvanishing order. We find

$$\varphi(\bar{\omega},\mathbf{k};\alpha^*=1/2)=\sqrt{1-\theta\eta\left(\frac{\mathbf{k}}{w}\right)^2}\,\bar{\omega}+\mathcal{O}(\bar{\omega}^2). \tag{4.36}$$

This through (4.34) specifies the leading singularity of the $G^R_{T_{xy}T_{xy}}(\omega,\mathbf{k})$ near ω_{11}. Substituting into (4.32), we then arrive at[14]

$$G^R_{T_{xy}T_{xy}}(t,\mathbf{k})\sim\frac{w^2}{\eta^{3/2}}\left[1-\theta\eta\left(\frac{\mathbf{k}}{w}\right)^2\right]^{\frac{1}{4}}e^{-i\left(1-\sqrt{1-\theta\eta\left(\frac{\mathbf{k}}{w}\right)^2}\right)\frac{w}{\theta}t}\times\int_{+i\infty+i\omega_{11}}^{-i\infty+i\omega_{11}}\frac{id\bar{\omega}}{2\pi}\sqrt{\bar{\omega}}e^{\omega t}. \tag{4.37}$$

The integration contour for this integral has been shown in black in the right panel of Fig. 7. We deform the contour across the branch cut of $\sqrt{\bar{\omega}}$ (blue in figure). Then we find

$$G^R_{T_{xy}T_{xy}}(t,\mathbf{k})\sim i\frac{w^2}{\eta^{3/2}}\left[1-\theta\eta\left(\frac{\mathbf{k}}{w}\right)^2\right]^{\frac{1}{4}}e^{-\left(1-\sqrt{1-\theta\eta\left(\frac{\mathbf{k}}{w}\right)^2}\right)\frac{w}{\theta}t}\times\int_{-\infty}^{0}\frac{d\bar{\omega}}{2\pi}\mathrm{Disc}\sqrt{\bar{\omega}}e^{\omega t}, \tag{4.38}$$

where $\mathrm{Disc}f(z)=\lim_{\epsilon\to0}f(z+i\epsilon)-f(z-i\epsilon)$. Performing the above integral we find

$$\boxed{G^R_{T_{xy}T_{xy}}(t,\mathbf{k})\sim w^{1/2}\left[1-\theta\eta\left(\frac{\mathbf{k}}{w}\right)^2\right]^{\frac{1}{4}}\frac{e^{-\left(1-\sqrt{1-\theta\eta\left(\frac{\mathbf{k}}{w}\right)^2}\right)\frac{w}{\theta}t}}{(\gamma_\eta t)^{3/2}}}, \tag{4.39}$$

with $\gamma_\eta=\eta/w$. This is the central result of this subsection; it can only be used to describe the decay of correlation function at times larger than the "diffusion time." As mentioned earlier, the rate of transverse momentum diffusion is given by the expression in front of t in the exponential, that we call it Γ_D. Then the diffusion time is defined as

$$t_D\equiv\Gamma_D^{-1}=\left[\left(1-\sqrt{1-\theta\eta\left(\frac{\mathbf{k}}{w}\right)^2}\right)\frac{w}{\theta}\right]^{-1}. \tag{4.40}$$

[14]The prefactor $\frac{w^2}{\eta^{3/2}}$ in (4.37) has two parts; w^2 comes from (4.5) while $1/\eta^{3/2}$ comes from the "constant" sitting in front of (4.34).

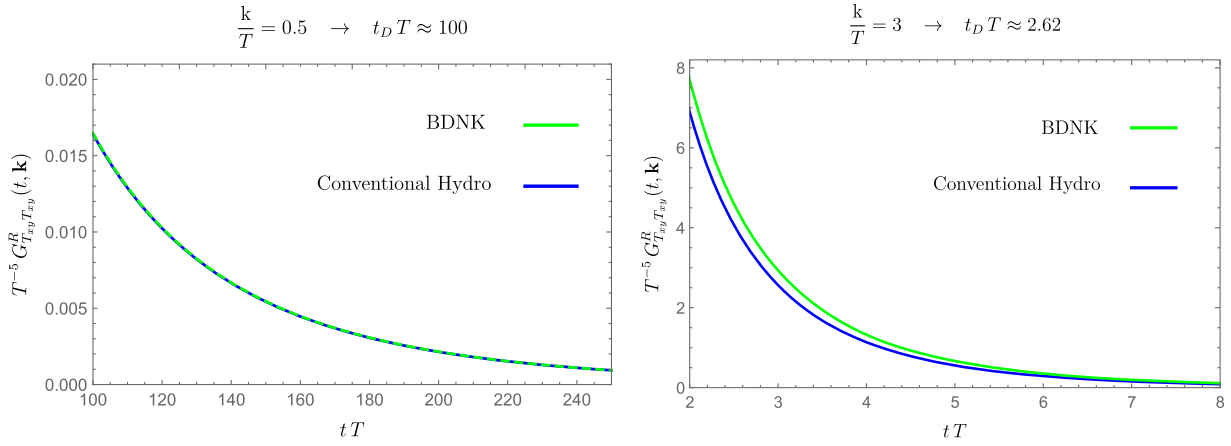

FIG. 8. Long-time tail comparison between BDNK and the conventional first-order relativistic hydrodynamics for $\frac{\theta}{s} = \frac{4\eta}{s} = \frac{1}{\pi}$. Both panels have been illustrated for times larger than the diffusion time of the transverse momentum, i.e., $t \gtrsim t_D$. Left panel: for relatively small momenta, nonlinear effects in BDNK theory are consistent with the same effects in the conventional hydro. Right panel: at large momentum, the nonlinear effects in BDNK theory lead to slower decay of the response function than those in conventional hydro.

It is worth emphasizing that in the conventional hydrodynamics, $\theta = 0$. In this case (4.39) becomes

$$G^R_{T_{xy}T_{xy}}(t, \mathbf{k}) \sim w^{1/2} \frac{e^{-\frac{1}{2}\gamma_\eta \mathbf{k}^2 t}}{(\gamma_\eta t)^{3/2}}. \tag{4.41}$$

As one expects, there is a tail with fractional power together with an exponentially decaying factor [56]. The decay of the exponential factor is controlled by $\frac{1}{2}\gamma_\eta \mathbf{k}^2$ which is familiar from conventional hydro [56]. In another familiar limit, we can reproduce the well-known result of [36] at zero momentum:

$$G^R_{T_{xy}T_{xy}}(t, \mathbf{k} = 0) \sim \frac{w^{1/2}}{(\gamma_\eta t)^{3/2}}. \tag{4.42}$$

This is the same as Eq. (42) in the mentioned reference.

In order to gain more insight about the difference between BDNK theory and conventional hydrodynamics, we proceed with illustrating behavior of $G^R_{T_{xy}T_{xy}}(t, \mathbf{k})$ for both cases in Fig. 8. In order to explain how we have chosen the values of k in the figure, let us recall the dispersion relations in the linear regime (4.6). As mentioned around Fig. 2, for $\theta_\eta = 4$, the range of validity of BDNK theory is $\mathfrak{q} \lesssim 0.5$. In terms of dimensionful quantities, it is written as [see (3.4)]

$$\frac{\mathrm{k}}{T} \lesssim \frac{1}{8}\left(\frac{\eta}{s}\right)^{-1}. \tag{4.43}$$

Motivated by the value of η/s frequently used for quark gluon plasma, we set $\frac{\eta}{s} = \frac{1}{4\pi}$. Then (4.43) simply tells us that we can use momenta within the range $\frac{\mathrm{k}}{T} \lesssim \frac{\pi}{2}$. For illustrative purposes, we have taken two different values for $\frac{\mathrm{k}}{T}$, one from this range and another from outside of this range: $\frac{\mathrm{k}}{T} = 0.5$ and 3. The corresponding diffusion times can be found from (4.40). It turns out that for BDNK theory $t_D T \approx 100, 2.62$, respectively. For conventional hydro, with $\theta = 0$, the corresponding values are found to be very close to these values. So we take the same values of t_D, namely $t_D T \approx 100$, 2.62, for the two corresponding conventional hydro cases. Then for each choice of k, we show the decay of correlation function within the range $t \gtrsim t_D$.

As is seen in the figure,

(1) At a small value of $\frac{\mathrm{k}}{T}$, the BDNK results are indistinguishable from the long-time tail caused by nonlinear effects in conventional hydrodynamics. Although the same result for the linear effects at small momentum could be predicted, the current result shows that at small momenta, even nonlinearities are not sensitive to UV physics. This can also be checked by taking the small momentum limit in (4.39)

$$\lim_{\mathrm{k}/T \to 0} G^R_{T_{xy}T_{xy}}(t, \mathbf{k}) \sim w^{1/2} \frac{e^{-\frac{1}{2}\gamma_\eta \mathbf{k}^2 t}}{(\gamma_\eta t)^{3/2}}. \tag{4.44}$$

The result is the same as if θ were zero [see (4.41)]. We see that θ vanishes from the nonlinear results corresponding to the small momentum limit.

(2) At momenta outside the range of validity of BDNK theory, the effect of UV regulator is significant. As shown in the right panel of the figure, the decay of correlation function in BDNK theory decays more slowly than the correlation function in conventional hydrodynamics. This is of course due to the action of the UV regulator θ, which weakens diffusion of the

transverse momentum. It can be simply understood by comparing ω_{11} within two theories:

$$\text{Conventional hydro:} \qquad \omega_{11} = -\frac{i}{2}\frac{\eta}{w}\mathbf{k}^2 \tag{4.45}$$

$$\text{BDNK:} \qquad \omega_{11} = -i\left(1 - \sqrt{1 - \theta\eta\left(\frac{\mathbf{k}}{w}\right)^2}\right)\frac{w}{\theta}. \tag{4.46}$$

We see that θ pushes ω_{11} in (4.45) away from the real axis in the lower half complex ω plane. It should be noted that this is just a mathematical result; the BDNK theory is not supposed to give reliable results at large momenta.[15]

V. DISCUSSION AND OUTLOOK

This work focuses on correlation functions in BDNK theory, especially in conformal systems. The first part of this work focuses on the derivation of momentum space correlation functions in the sound and shear channels. The pole structure of the correlation functions is analyzed and found to be consistent with the spectrum discovered by studying the linearized BDNK equations in [16]. Our calculations also reveal this feature of the theory that the correlation function of the energy density develops a range of negative values. It should be noted that this feature is not the case in the small momentum limit, where we expect the theory to be consistent with conventional hydrodynamics.

In order to gain insight about nonlinear fluctuations in the theory we borrowed some methods from field theory to find the structure of the correlation function outside the linear response regime. By developing a numerical method for solving the on shell conditions, we discovered the branch-cut structure of the shear stress response function. We also solved the Landau equations analytically to find the threshold singularities of the same response function. To the best of our knowledge, this is the first time these ideas have been introduced and applied in a hydrodynamics framework. It would be interesting to extend this analysis to the sound channel, where one would hope to see a richer structure of correlation functions.

To understand how the branch point singularities discovered above affect the real-space correlation function, we then investigated the late-time behavior of the stress tensor correlation function. We calculated the long-time tail of this correlation function. Consistent with conventional hydrodynamics [36], we found a tail with the fractional power $\sim t^{-3/2}$ with an exponential decay factor. Although the tail $\sim t^{-3/2}$ does not exhibit any specific characteristics of BDNK theory, the exponential decay factor depends on the parameter θ of BDNK theory. However, it turns out that in the small momentum limit the U regulator θ vanishes from the exponential decay factor; in other words, the U regulator does not affect the late-time hydrodynamic evolution. It would be interesting to study the late-time behavior of the correlation functions in nonequilibrium settings [57–61].

Regarding the correlation functions in the nonlinear regime, it would be very interesting to construct an effective field theory corresponding to the stable first-order hydrodynamics. In this way, interactions between hydrodynamic modes can be considered systematically. Some initial steps in this direction have recently been taken in Ref. [42]. The theory of UV-regulated nonlinear diffusion constructed in Ref. [42] can be regarded as the effective field theory of transverse channel velocity fluctuations. A more general treatment requires including fluctuations of the temperature as well as the longitudinal component of the fluid velocity. We hope we turn to this issue in the future. In a more systematic way, using the EFT ideas developed in [62], it would be interesting to construct the Schwinger-Keldysh EFT associated with the BDNK theory. See [63,64] for related recent works.

ACKNOWLEDGMENTS

We thank Lorenzo Gavassino, Matthias Kaminski, and Omid Tavakol for valuable discussions and comments. We especially thank Pavel Kovtun for discussions on Ref. [16] and Hofie S. Hannesdottir for discussing Ref. [53]. N. A. was supported by Grant No. 561119208 "Double First Class" start-up funding of Lanzhou University, China. S. T. was supported by Younger Scientist Scholarship QN2021043004 with the funding number E11I631KR0.

APPENDIX A: EQUILIBRIUM FLUCTUATIONS

The problem of finding the mean value of quantities in equilibrium can be studied via finding the probability distribution of their deviations from the associated mean values [40]. In the simplest setting, quantities of interest are energy density and momentum density. What we need then is to exploit a fundamental property of entropy: the probability of finding a subsystem at energy density $\mathcal{E}$ and momentum density $\mathcal{P}$ is given in terms of the total entropy of the system together with the medium, S_t, and also with its change in fluctuations:

$$\mathrm{w}(\mathcal{E}, \mathcal{P}_i) \sim e^{S_t} \sim e^{\Delta S_t} \sim e^{-\int_{\mathrm{x}} \mathcal{R}/T}, \tag{A1}$$

[15]We thank Pavel Kovtun for discussion on this point.

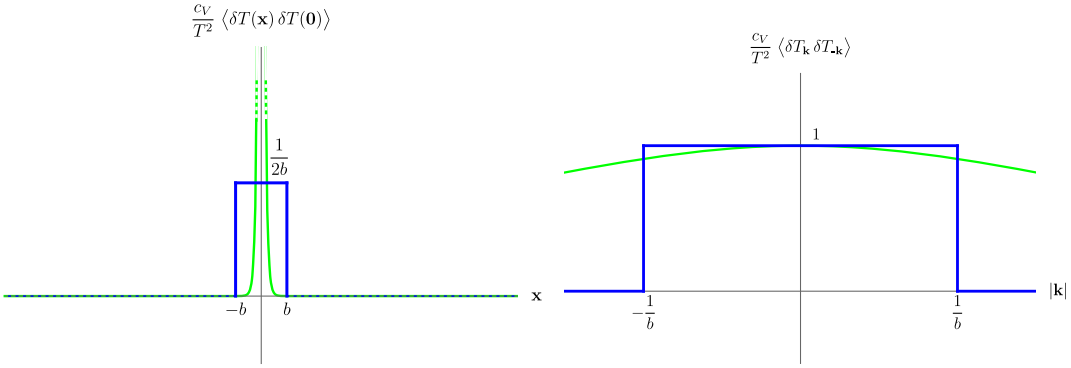

FIG. 9. Illustration of equal-time correlation function of the temperature fluctuations (in one dimension). Left: position space; Right: momentum space. Here b shows the size of the hydrodynamic cell, and $\Lambda = 1/b$ is the UV cutoff of the hydrodynamic theory. In the limit, $b \to 0$, the blue functions in left and right become $\delta(\mathbf{x})$ and 1, respectively. This corresponds to (A4a). The green curves in left and right correspond to (A8a) and (A9a), respectively.

where $\mathcal{R} = \Delta\mathcal{E} - \mathbf{v}\cdot\Delta\boldsymbol{\mathcal{P}} - T\Delta\mathcal{S}$, with $\mathbf{v}$ and T being the equilibrium (mean) values of the velocity and the temperature of the system. $\Delta\mathcal{E}$, $\Delta\boldsymbol{\mathcal{P}}$, and $\Delta\mathcal{S}$ are the fluctuations of energy density, momentum density and the entropy density. Expanding the latter to second order in terms of the former two ones, and using the fact that first derivatives vanish in equilibrium, we find

$$\frac{\mathcal{R}}{T} = \frac{1}{2}\left[-\delta\left(\frac{1}{T}\right)\Delta\mathcal{E} + \delta\left(\frac{\mathbf{v}}{T}\right)\cdot\Delta\boldsymbol{\mathcal{P}}\right], \tag{A2}$$

where δ and Δ indicate the fluctuation in source and the fluctuation in energy/momentum density, respectively. For a fluid at rest, $\Delta\mathcal{E} = c_V\delta T$ and $\Delta\boldsymbol{\mathcal{P}} = w\delta\mathbf{v}$. Therefore (A2) becomes

$$\frac{\mathcal{R}}{T} = \frac{1}{2}\left[\frac{c_V}{T^2}(\delta T)^2 + \frac{w}{T}(\delta\mathbf{v})^2\right]. \tag{A3}$$

From this one can immediately read the thermal fluctuations in the system. As it is explicitly expressed in Ref. [40], "calculation of correlation functions of fluctuations in a fluid at rest calls for no special study: these are described as the usual thermal fluctuations." Therefore in a fluid at rest, we find the "equal-time" correlation functions as the following [41][16]:

$$\langle\delta T(\mathbf{x}_1)\delta T(\mathbf{x}_2)\rangle = \frac{T^2}{c_V}\delta^3(\mathbf{x}_1 - \mathbf{x}_2) \tag{A4a}$$

$$\langle\delta v_i(\mathbf{x}_1)\delta v_j(\mathbf{x}_2)\rangle = \delta_{ij}\frac{T}{w}\delta^3(\mathbf{x}_1 - \mathbf{x}_2), \tag{A4b}$$

$$\langle\delta T(\mathbf{x}_1)\delta v_j(\mathbf{x}_2)\rangle = 0. \tag{A4c}$$

To gain a deeper understanding of the above correlation functions, let us review the discussion at the beginning of Sec. IV. We assume that the macroscopic fields change on a scale of order L. Since the system is at rest, L must be infinite; however, for future purposes, we treat it as finite but very large compared to b, i.e. the hydrodynamic cell size: $L \gg b$. The length b must also be much larger than the microscopic length scale $1/T$: $b \gg 1/T$. Therefore, we have [48]

$$\ell_{\text{mic}} \sim \frac{1}{T} \ll b \ll L. \tag{A5}$$

The above separation of scales clearly shows the "physical" meaning of the equal-time correlation functions in (A4a) and (A4b): whereas mathematically they are represented by the Dirac delta function, which is expected to be zero for any $|\mathbf{x}_1 - \mathbf{x}_2| \neq 0$, they are just zero for $|\mathbf{x}_1 - \mathbf{x}_2| \gtrsim b$. When the two points are close enough and located within a hydro cell, i.e. $|\mathbf{x}_1 - \mathbf{x}_2| \lesssim b$, the two correlation functions take constant values over the entire cell. See the blue function in the left panel of Fig. 9. In the limit $b \to 0$, the mathematical results given by (A4a) and (A4b) are recovered.

Before concluding this subsection, we would like to emphasize that $\delta T(\mathbf{x})$ and $\delta v_i(\mathbf{x})$ determine the fluctuations in temperature and velocity near equilibrium. However, as discussed in the Introduction, these quantities are not well defined in nonequilibrium conditions. One might think of choosing different definitions for them, similar to the choice of frames in hydrodynamics. This may affect the results presented in (A4a)–(A4c), and ultimately the

[16]We would like to thank Lorenzo Gavassino for discussions on these equations. According to our private correspondence, he and his collaborators are preparing a work that is an improved version of the entire discussion in this section. This way, they will be able to mathematically circumvent the features observed in Fig. 1. See also the discussion about "information current" in Ref. [65] and the excellent discussion in Sec. II of Ref. [64].

hydrodynamic correlation functions in the next subsection.[17] Below, we will elaborate on this in detail.

Let us investigate the behavior of equal-time correlation functions under a general change in the definition of out of equilibrium temperature and velocity, caused by first-order derivative corrections. We consider the following transformation:

$$\frac{\delta T}{T} \to \frac{\delta T}{T} + \frac{a_1}{T}\boldsymbol{\nabla}\cdot\delta\mathbf{v}$$
$$\delta\mathbf{v} \to \delta\mathbf{v} + \frac{a_2}{T}\boldsymbol{\nabla}\left(\frac{\delta T}{T}\right), \tag{A6}$$

where a_1 and a_2 are two dimensionless parameters. Considering (A5), the derivative terms in (A6) are of order $1/LT \ll 1$.

Applying transformations (A6) to (A3), $\mathcal{R}$ takes the following form in momentum space:

$$\int_{\mathbf{x}}\frac{\mathcal{R}}{T} = \int_{\mathbf{k}}\frac{1}{2}\left[\left(\frac{c_V}{T^2}+\frac{a_2^2 w}{T^5}\mathbf{k}^2\right)\delta T_{\mathbf{k}}\delta T_{-\mathbf{k}} + \left(\frac{w}{T}+\frac{a_1^2 c_V}{T^2}\mathbf{k}^2\right)\delta\mathbf{v}_{\mathbf{k}}\cdot\delta\mathbf{v}_{-\mathbf{k}}\right], \tag{A7}$$

from which we find

$$\langle\delta T_{\mathbf{k}}\delta T_{-\mathbf{k}}\rangle = \frac{T^2}{c_V}\frac{1}{1+\left(\frac{a_2^2 w}{c_V T^3}\right)\mathbf{k}^2}, \tag{A8a}$$

$$\langle\delta v^i_{\mathbf{k}}\delta v^j_{-\mathbf{k}}\rangle = \delta_{ij}\frac{T}{w}\frac{1}{1+\left(\frac{a_1^2 c_V}{wT}\right)\mathbf{k}^2}, \tag{A8b}$$

$$\langle\delta T_{\mathbf{k}}\delta v^j_{-\mathbf{k}}\rangle = 0. \tag{A8c}$$

In order to express the above result in a form similar to (A4a) and (A4b), we now proceed to find the inverse Fourier transform. We find:

$$\langle\delta T(\mathbf{x}_1)\delta T(\mathbf{x}_2)\rangle = \frac{T^2}{c_V}\frac{1}{4\pi\xi_2^2}\frac{1}{|\mathbf{x}_1-\mathbf{x}_2|}e^{-|\mathbf{x}_1-\mathbf{x}_2|/\xi_2}, \tag{A9a}$$

$$\langle\delta v_i(\mathbf{x}_1)\delta v_j(\mathbf{x}_2)\rangle = \delta_{ij}\frac{T}{w}\frac{1}{4\pi\xi_1^2}\frac{1}{|\mathbf{x}_1-\mathbf{x}_2|}e^{-|\mathbf{x}_1-\mathbf{x}_2|/\xi_1}, \tag{A9b}$$

$$\langle\delta T(\mathbf{x}_1)\delta v_j(\mathbf{x}_2)\rangle = 0, \tag{A9c}$$

where ξ_1 and ξ_2 are two microscopic length scales defined as

$$\xi_1 = a_1\left(\frac{c_V}{wT}\right)^{1/2}, \qquad \xi_2 = a_2\left(\frac{w}{c_V T^3}\right)^{1/2}. \tag{A10}$$

Note that the transformation (A6) keeps the correlation functions diagonal; i.e. the cross-correlator $\langle\delta T\delta v_j\rangle$ still vanishes.

In conformal fluids, $\xi_{1,2} \sim \frac{a_{1,2}}{T}$. Therefore, as it is shown in the left panel of Fig. 9, for finite nonzero values of a_1 and a_2[18]

(1) The exponential factors in (A9a) and (A9b) are of order $e^{-|\mathbf{x}_1-\mathbf{x}_2|T}$ and vanish at distances $|\mathbf{x}_1-\mathbf{x}_2| \gtrsim b$, consistent with (A4a) and (A4b) [41].
(2) At shorter distances, i.e. $|\mathbf{x}_1-\mathbf{x}_2| \lesssim b$, which is actually beyond the regime of validity of hydro, $e^{-|\mathbf{x}_1-\mathbf{x}_2|T}$ is nonvanishing, but is not constant.

We see that applying the transformations (A6) regulates the equilibrium correlation functions at distances smaller than the hydro cell size; the Dirac delta functions in (A4a) and (A4b) (taken as constant values within a cell) transform to (A9a) and (A9b) that are actually exponentially decaying functions within the cell.[19] It would be interesting to investigate the effect of this regularization of equilibrium correlation functions on the hydrodynamic correlation functions.

APPENDIX B: HYDRODYNAMIC FLUCTUATIONS

Now let us move on to study the "different-time" correlation functions $\langle\delta\phi_a(t,\mathbf{x})\delta\phi_b(0,\mathbf{0})\rangle$. It is easy to show that

$$\langle\delta\phi_a\delta\phi_b\rangle_{\omega\mathbf{k}} = \langle\delta\phi_a\delta\phi_b\rangle^{(+)}_{\omega\mathbf{k}} + \langle\delta\phi_b\delta\phi_a\rangle^{(+)}_{-\omega-\mathbf{k}}, \tag{B1}$$

where $\langle\delta\phi_a\delta\phi_b\rangle^{(+)}_{\omega\mathbf{k}}$ is a one-sided Fourier transformation of $\langle\delta\phi_a(t,\mathbf{x})\delta\phi_b(0,\mathbf{0})\rangle$, defined as (3.3), but with the time integral taken from 0 to $+\infty$ [40,41]. The strategy is to find equations between one-sided Fourier transforms and then to calculate correlation functions by use of (B1).

We also take the momentum to be directed in the z direction $\mathfrak{q} = (0,0,q)$. This then allows us to calculate the correlation functions in two channels. In the longitudinal (sound) channel, the correlation functions of $\delta T/T$ and $\delta v^{\parallel} \equiv \delta v_z$ are involved. In the transverse (shear) channel, only $\langle\delta v^{\perp}\delta v^{\perp}\rangle$ needs to be computed.

1. Longitudinal channel

Multiplying the two equations (3.1) and the z component of (3.2) by $\delta T(0,\mathbf{0})$ from the right side, and averaging over

[17] We would like to thank the anonymous referee for pointing this out. Our following calculations and discussions are based on the referee recommendation given by (A6).

[18] It is easy to check that in the limit $a_1, a_2 \to 0$, (A9a) and (A9b) reduce to (A4a) and (A4b).

[19] We would like to thank Lorenzo Gavassino for privately sharing his results containing an equation similar to (A9a).

the local equilibrium, we find the equations of one-sided Fourier transformations as the following:

$$\left[-i\mathfrak{w}-\frac{1}{12}\left(\theta_\eta\mathfrak{q}^2+3\pi_\eta\mathfrak{w}^2\right)\right]\left\langle\frac{\delta T}{T}\frac{\delta T}{T}\right\rangle^{(+)}+\left[\frac{iq}{3}+\frac{1}{12}(\theta_\eta+\pi_\eta)q\mathfrak{w}\right]\left\langle\delta v_z\frac{\delta T}{T}\right\rangle^{(+)}=\frac{\bar{\eta}(4-i\pi_\eta\mathfrak{w})}{48\bar{p}^2T^4}$$
$$\left[-i\mathfrak{w}+\frac{1}{3}\mathfrak{q}^2-\frac{1}{12}\left(\pi_\eta\mathfrak{q}^2+3\theta_\eta\mathfrak{w}^2\right)\right]\left\langle\delta v_z\frac{\delta T}{T}\right\rangle^{(+)}+\left[iq+\frac{1}{4}(\theta_\eta+\pi_\eta)q\mathfrak{w}\right]\left\langle\frac{\delta T}{T}\frac{\delta T}{T}\right\rangle^{(+)}=0. \tag{B2}$$

Note that the right side of the first equation above is the consequence of using (A4a). When multiplying (3.1) and the z component of (3.2) by $\delta v_z(0,\mathbf{0})$, and repeating the above process, we arrive at

$$\left[-i\mathfrak{w}-\frac{1}{12}\left(\theta_\eta\mathfrak{q}^2+3\pi_\eta\mathfrak{w}^2\right)\right]\left\langle\frac{\delta T}{T}\delta v_z\right\rangle^{(+)}+\left[\frac{iq}{3}+\frac{1}{12}(\theta_\eta+\pi_\eta)q\mathfrak{w}\right]\langle\delta v_z\delta v_z\rangle^{(+)}=0$$
$$\left[-i\mathfrak{w}+\frac{1}{3}\mathfrak{q}^2-\frac{1}{12}\left(\pi_\eta\mathfrak{q}^2+3\theta_\eta\mathfrak{w}^2\right)\right]\langle\delta v_z\delta v_z\rangle^{(+)}+\left[iq+\frac{1}{4}(\theta_\eta+\pi_\eta)q\mathfrak{w}\right]\left\langle\frac{\delta T}{T}\delta v_z\right\rangle^{(+)}=\frac{\bar{\eta}(4-i\theta_\eta\mathfrak{w})}{16\bar{p}^2T^4}. \tag{B3}$$

From these equations we find

$$\left\langle\frac{\delta T}{T}\frac{\delta T}{T}\right\rangle^{(+)}=\frac{\bar{\eta}}{4\bar{p}^2T^4}\frac{1}{\mathcal{D}_L(\mathfrak{w},\mathfrak{q})}(i\pi_\eta\mathfrak{w}-4)\left((\pi_\eta-4)\mathfrak{q}^2+12i\mathfrak{w}+3\theta_\eta\mathfrak{w}^2\right) \tag{B4a}$$

$$\left\langle\delta v_z\frac{\delta T}{T}\right\rangle^{(+)}=\frac{3\bar{\eta}}{4\bar{p}^2T^4}\frac{1}{\mathcal{D}_L(\mathfrak{w},\mathfrak{q})}iq(i\pi_\eta\mathfrak{w}-4)\left(4-i(\theta_\eta+\pi_\eta)\mathfrak{w}\right) \tag{B4b}$$

$$\left\langle\frac{\delta T}{T}\delta v_z\right\rangle^{(+)}=\frac{3\bar{\eta}}{4\bar{p}^2T^4}\frac{1}{\mathcal{D}_L(\mathfrak{w},\mathfrak{q})}iq(i\theta_\eta\mathfrak{w}-4)\left(4-i(\theta_\eta+\pi_\eta)\mathfrak{w}\right) \tag{B4c}$$

$$\langle\delta v_z\delta v_z\rangle^{(+)}=\frac{3\bar{\eta}}{4\bar{p}^2T^4}\frac{1}{\mathcal{D}_L(\mathfrak{w},\mathfrak{q})}(i\theta_\eta\mathfrak{w}-4)(\theta_\eta\mathfrak{q}^2+12i\mathfrak{w}+3\pi_\eta\mathfrak{w}^2) \tag{B4d}$$

with

$$\mathcal{D}_L(\mathfrak{w},\mathfrak{q})=9\pi_\eta\theta_\eta\mathfrak{w}^4+36i(\theta_\eta+\pi_\eta)\mathfrak{w}^3-6(\pi_\eta(\theta_\eta+2)\mathfrak{q}^2+24)\mathfrak{w}^2$$
$$-12i(\theta_\eta+\pi_\eta+4)\mathfrak{q}^2\mathfrak{w}+\left((\pi_\eta-4)\theta_\eta\mathfrak{q}^2+48\right)\mathfrak{q}^2. \tag{B5}$$

Then it is easy to calculate the correlation functions by using (B1). We do not represent those expressions here explicitly.

2. Transverse channel

Owing to the rotational symmetry in the transverse plane, we only need to consider the x component of (3.2). Multiplying by $\delta v_x(0,\mathbf{0})$, the one-sided Fourier transformation of $\langle\delta v_x(t,\mathbf{x})\delta v_x(0,\mathbf{0})\rangle$ is found to be

$$\langle\delta v_i\delta v_i\rangle^{(+)}=\frac{i\bar{\eta}}{4\bar{p}^2T^4}\frac{4i\gamma+\mathfrak{w}+\gamma^2(\theta_\eta-1)\mathfrak{w}}{\mathcal{D}_T(\mathfrak{w},\mathfrak{q})}\,i=x,y, \tag{B6}$$

where $\mathcal{D}_T$ is given in the main text. Again, it is easy to calculate $\langle\delta v_i\delta v_i\rangle$ by using (B1).

APPENDIX C: LANDAU EQUATIONS

In this appendix we briefly review how to use the Landau equations to find the singularities of a Feynman diagram.

1. Threshold singularities

Let us suppose an arbitrary Feynman diagram (in the scalar theory) is represented by the following integral:

$$\mathcal{I}(p)=\int\frac{d^4k}{(2\pi)^4}\frac{d^4l}{(2\pi)^4}\cdots\frac{B}{A_1A_2\cdots}, \tag{C1}$$

where $A_i=q_i^2+m^2$ and q_i is the four-momentum corresponding to the given line in the diagram. In addition, B is a polynomial of the four-vectors q_i. Using the well-known "Feynman parameters" method, one may write

$$\frac{1}{A_1A_2\cdots A_n}=(n-1)!\int_0^1\int_0^1\cdots\int_0^1\frac{d\alpha_1 d\alpha_2\cdots d\alpha_n\delta(\alpha_1+\alpha_2+\cdots+\alpha_n-1)}{(\alpha_1A_1+\alpha_2A_2+\cdots\alpha_nA_n)^n}. \tag{C2}$$

Landau argues that the singularities of the integral (C1)[20] are actually a solution to the following equations/conditions [49]:

(1) For each propagator $i=1,\ldots,n$:

$$q_i^2+m^2=0 \quad \text{or} \quad \alpha_i=0. \tag{C3}$$

(2) For each loop momentum integration variable k_j:

$$\frac{\partial}{\partial k_j}\sum_i\alpha_i(q_i^2+m^2)=0. \tag{C4}$$

These conditions are referred to as the "*Landau equations*" or "*Landau conditions*." The first condition, (C3), is simply the on shell condition for the internal momenta. These on shell conditions identify where singularities can occur in the integrand in a Feynman integral, which is a necessary but not a sufficient condition for a singularity to develop in the full integral [53]. The second one, given by (C4), is called the "Landau loop equation." We explain it below.

To understand (C4), let us denote that the singularity of the integrand will be the singularity of the integral if it cannot be avoided by doing any contour deformation. One way to achieve this is that, by changing the external momentum, the singularity of the integrand reaches the endpoint of the integration; the latter is called "*end-point singularity*" which is actually quite easy to identify. Another possibility is that, for a given set of external momenta, the contour of integration is pinched between singularities of the integrand at some real value of the loop momentum. Remember when two curves are tangent, their normal vectors at the point of intersection are parallel. Similarly, there will be a contour pinch when the gradients of the on shell conditions (with respect to the independent loop momenta) are linearly dependent. The latter singularity is called "*pinch singularity*" [53,55].[21]

It should be noted that solutions to the Landau equations that require some Feynman parameters α_i to be either negative or complex do not correspond to singularities of $\mathcal{I}(p)$ that can be accessed with real on shell *external* momenta [53]. The latter momenta define the *physical region*. On the other hand, when $\mathcal{I}(p)$ is multivalued, one can be in the physical region on different Riemann sheets:

(1) The entire set of complex points accessible through the analytic continuation of the physical region defines the *physical sheet*. Singularities associated with positive Feynman parameters ($\alpha_i>0$) are on the physical sheet and are called *normal threshold singularities*.

(2) Singularities associated with negative or complex values of the Feynman parameters are not on the physical sheet and are called *pseudothreshold singularities*.

The above singularities are all called *first-type Landau singularities*. As we saw, for this class of singularities the notion of threshold in the space of external variables is well-defined. The Landau equations however can also describe singularities at infinite loop momenta. Remember the fourth comment below (4.12). We saw that the two singularities $\mathfrak{w}_{12}$ and $\mathfrak{w}_{21}$ were of this type. Sometimes they are referred to as *second-type singularities* [55].

2. Nature of singularities

Let us combine (C1) and (C2):

$$\mathcal{I}(p)=(n-1)!\int\frac{d^dk}{(2\pi)^d}\frac{d^dl}{(2\pi)^d}\cdots\int_0^1\int_0^1\cdots \times\int_0^1\frac{d\alpha_1\cdots d\alpha_n\delta(\alpha_1+\cdots+\alpha_n-1)}{f^n}, \tag{C5}$$

where $f=\alpha_1A_1+\cdots\alpha_nA_n$. Let us call the solutions to the Landau-loop equations α^*. Landau argues that leading singularity of $\mathcal{I}(p)$ is given by

$$\sim(f(p,\alpha^*))^{\frac{1}{2}m-n}, \tag{C6}$$

where m is the number of independent integrations in $\mathcal{I}(p)$ and n is the number of internal lines in the Feynman diagram.

(1) The number of momentum integration in d dimension is $d\nu$ where ν is the number of independent contour. Clearly, $\nu=n-V+1$ with V being the number of vertices in the diagram. Thus the number of momentum integration in the d dimension is $d(n-V+1)$.

(2) There are $n-1$ of α integrations.

Therefore, m, the total number of independent integrations is given by

$$m=d(n-V+1)+(n-1). \tag{C7}$$

Instead of the number of contours, it is more convenient to represent it in terms of the number of vertices V. It then reads as

$$\sim(f(p,\alpha^*))^{\frac{d-1}{2}(n+1)-\frac{d}{2}V}. \tag{C8}$$

[20]These singularities include both normal (discussed in this paper) and anomalous thresholds. For anomalous thresholds see [66,67].

[21]See also [68,69].

[1] P. Kovtun, Lectures on hydrodynamic fluctuations in relativistic theories, J. Phys. A **45**, 473001 (2012).

[2] C. Eckart, The thermodynamics of irreversible processes. 3. Relativistic theory of the simple fluid, Phys. Rev. **58**, 919 (1940).

[3] L. D. Landau and E. M. Lifshitz, *Fluid Mechanics*, Course of Theoretical Physics Vol. 6 (Elsevier Science, New York, 2013).

[4] W. A. Hiscock and L. Lindblom, Generic instabilities in first-order dissipative relativistic fluid theories, Phys. Rev. D **31**, 725 (1985).

[5] W. A. Hiscock and L. Lindblom, Linear plane waves in dissipative relativistic fluids, Phys. Rev. D **35**, 3723 (1987).

[6] W. Israel, Nonstationary irreversible thermodynamics: A causal relativistic theory, Ann. Phys. (N.Y.) **100**, 310 (1976).

[7] W. Israel and J. M. Stewart, Thermodynamics of nonstationary and transient effects in a relativistic gas, Phys. Lett. **58A**, 213 (1976).

[8] M. Luzum and P. Romatschke, Conformal relativistic viscous hydrodynamics: Applications to RHIC results at $\sqrt{S_{NN}} = 200 \times$ GeV, Phys. Rev. C **78**, 034915 (2008); **79**, 039903(E) (2009).

[9] R. Baier, P. Romatschke, D. T. Son, A. O. Starinets, and M. A. Stephanov, Relativistic viscous hydrodynamics, conformal invariance, and holography, J. High Energy Phys. 04 (2008) 100.

[10] G. S. Denicol, H. Niemi, E. Molnar, and D. H. Rischke, Derivation of transient relativistic fluid dynamics from the Boltzmann equation, Phys. Rev. D **85**, 114047 (2012); **91**, 039902(E) (2015).

[11] W. Florkowski, M. P. Heller, and M. Spalinski, New theories of relativistic hydrodynamics in the LHC era, Rep. Prog. Phys. **81**, 046001 (2018).

[12] C. Shen and L. Yan, Recent development of hydrodynamic modeling in heavy-ion collisions, Nucl. Sci. Tech. **31**, 122 (2020).

[13] P. Van and T. S. Biro, First order and stable relativistic dissipative hydrodynamics, Phys. Lett. B **709**, 106 (2012).

[14] H. Freistuhler and B. Temple, Causal dissipation for the relativistic dynamics of ideal gases, Proc. R. Soc. A **473**, 0729 (2017).

[15] F. S. Bemfica, M. M. Disconzi, and J. Noronha, Causality and existence of solutions of relativistic viscous fluid dynamics with gravity, Phys. Rev. D **98**, 104064 (2018).

[16] P. Kovtun, First-order relativistic hydrodynamics is stable, J. High Energy Phys. 10 (2019) 034.

[17] F. S. Bemfica, M. M. Disconzi, and J. Noronha, First-order general-relativistic viscous fluid dynamics, Phys. Rev. X **12**, 021044 (2022).

[18] F. S. Bemfica, F. S. Bemfica, M. M. Disconzi, M. M. Disconzi, J. Noronha, and J. Noronha, Nonlinear causality of general first-order relativistic viscous hydrodynamics, Phys. Rev. D **100**, 104020 (2019); **105**, 069902(E) (2022).

[19] R. E. Hoult and P. Kovtun, Stable and causal relativistic Navier-Stokes equations, J. High Energy Phys. 06 (2020) 067.

[20] S. Mitra, Causality and stability analysis of first-order field redefinition in relativistic hydrodynamics from kinetic theory, Phys. Rev. C **105**, 054910 (2022).

[21] R. E. Hoult and P. Kovtun, Causal first-order hydrodynamics from kinetic theory and holography, Phys. Rev. D **106**, 066023 (2022).

[22] J. Armas and F. Camilloni, A stable and causal model of magnetohydrodynamics, J. Cosmol. Astropart. Phys. 10 (2022) 039.

[23] M. Shokri and D. H. Rischke, Linear stability analysis in inhomogeneous equilibrium configurations, Phys. Rev. D **108**, 096029 (2023).

[24] R. Biswas, S. Mitra, and V. Roy, Is first-order relativistic hydrodynamics in a general frame stable and causal for arbitrary interactions?, Phys. Rev. D **106** (2022), L011501.

[25] M. Shokri and F. Taghinavaz, Conformal Bjorken flow in the general frame and its attractor: Similarities and discrepancies with the Müller-Israel-Stewart formalism, Phys. Rev. D **102**, 036022 (2020).

[26] A. Das, W. Florkowski, J. Noronha, and R. Ryblewski, Equivalence between first-order causal and stable hydrodynamics and Israel-Stewart theory for boost-invariant systems with a constant relaxation time, Phys. Lett. B **806**, 135525 (2020).

[27] A. Das, W. Florkowski, and R. Ryblewski, Correspondence between Israel-Stewart and first-order causal and stable hydrodynamics for the boost-invariant massive case with zero baryon density, Phys. Rev. D **102**, 031501 (2020).

[28] H. Freistuhler, Nonexistence and existence of shock profiles in the Bemfica-Disconzi-Noronha model, Phys. Rev. D **103**, 124045 (2021).

[29] A. Daher, A. Das, and R. Ryblewski, Stability studies of first order spin-hydrodynamic frameworks, Phys. Rev. D **107**, 054043 (2023).

[30] T. Dore, L. Gavassino, D. Montenegro, M. Shokri, and G. Torrieri, Fluctuating relativistic dissipative hydrodynamics as a gauge theory, Ann. Phys. (Amsterdam) **442**, 168902 (2022).

[31] L. Gavassino, Can we make sense of dissipation without causality?, Phys. Rev. X **12**, 041001 (2022).

[32] L. Gavassino, M. Antonelli, and B. Haskell, When the entropy has no maximum: A new perspective on the instability of the first-order theories of dissipation, Phys. Rev. D **102**, 043018 (2020).

[33] A. Pandya and F. Pretorius, Numerical exploration of first-order relativistic hydrodynamics, Phys. Rev. D **104**, 023015 (2021).

[34] H. Bantilan, Y. Bea, and P. Figueras, Evolutions in first-order viscous hydrodynamics, J. High Energy Phys. 08 (2022) 298.

[35] M. H. Ernst, E. H. Hauge, and J. M. J. van Leeuwen, Asymptotic time behavior of correlation functions, Phys. Rev. Lett. **25**, 1254 (1970).

[36] P. Kovtun and L. G. Yaffe, Hydrodynamic fluctuations, long time tails, and supersymmetry, Phys. Rev. D **68**, 025007 (2003).

[37] X. Chen-Lin, L. V. Delacrétaz, and S. A. Hartnoll, Theory of diffusive fluctuations, Phys. Rev. Lett. **122**, 091602 (2019).

[38] M. Martinez and T. Schäfer, Stochastic hydrodynamics and long time tails of an expanding conformal charged fluid, Phys. Rev. C **99**, 054902 (2019).

[39] L. P. Kadanoff and P. C. Martin, Hydrodynamic equations and correlation functions, Ann. Phys. (N.Y.) **24**, 419 (1963).

[40] L. D. Landau and E. M. Lifshitz, *Statistical Physics Part 1*, Course of Theoretical Physics Vol. 5 (Elsevier Science, New York, 2013).
[41] L. D. Landau and E. M. Lifshitz, *Statistical Physics Part 2*, Course of Theoretical Physics Vol. 9 (Elsevier Science, New York, 2013).
[42] N. Abbasi, M. Kaminski, and O. Tavakol, Ultraviolet-regulated theory of non-linear diffusion, arXiv:2212.11499.
[43] M. Crossley, P. Glorioso, and H. Liu, Effective field theory of dissipative fluids, J. High Energy Phys. 09 (2017) 095.
[44] K. Jensen, N. Pinzani-Fokeeva, and A. Yarom, Dissipative hydrodynamics in superspace, J. High Energy Phys. 09 (2018) 127.
[45] F. M. Haehl, R. Loganayagam, and M. Rangamani, Topological sigma models & dissipative hydrodynamics, J. High Energy Phys. 04 (2016) 39.
[46] H. Liu and P. Glorioso, Lectures on non-equilibrium effective field theories and fluctuating hydrodynamics, Proc. Sci. TASI2017 (**2018**) 008 [arXiv:1805.09331].
[47] P. Kovtun, G. D. Moore, and P. Romatschke, The stickiness of sound: An absolute lower limit on viscosity and the breakdown of second order relativistic hydrodynamics, Phys. Rev. D **84**, 025006 (2011).
[48] X. An, G. Basar, M. Stephanov, and H. U. Yee, Relativistic hydrodynamic fluctuations, Phys. Rev. C **100**, 024910 (2019).
[49] L. D. Landau, On analytic properties of vertex parts in quantum field theory, Nucl. Phys. **13**, 181 (1959).
[50] M. D. Schwartz, *Quantum Field Theory and the Standard Model* (Cambridge University Press, Cambridge, England, 2014), ISBN 978-1-107-03473-0, 978-1-107-03473-0.
[51] S. Endlich, A. Nicolis, R. Rattazzi, and J. Wang, The quantum mechanics of perfect fluids, J. High Energy Phys. 04 (2011) 102.
[52] B. Gripaios and D. Sutherland, Quantum field theory of fluids, Phys. Rev. Lett. **114**, 071601 (2015).
[53] H. S. Hannesdottir, A. J. McLeod, M. D. Schwartz, and C. Vergu, Constraints on sequential discontinuities from the geometry of on-shell spaces, J. High Energy Phys. 07 (2023) 236.
[54] D. B. Fairlie, P. V. Landshoff, J. Nuttall, and J. C. Polkinghorne, Singularities of the second type, J. Math. Phys. (N.Y.) **3**, 594 (1962).
[55] R. J. Eden, P. V. Landshoff, D. I. Olive, and J. C. Polkinghorne, *The Analytic S-Matrix* (Cambridge University Press, Cambridge, England, 1966).
[56] L. V. Delacretaz, Heavy operators and hydrodynamic tails, SciPost Phys. **9**, 034 (2020).
[57] Y. Bu and M. Lublinsky, All order linearized hydrodynamics from fluid-gravity correspondence, Phys. Rev. D **90**, 086003 (2014).
[58] Y. Bu and M. Lublinsky, Linearized fluid/gravity correspondence: From shear viscosity to all order hydrodynamics, J. High Energy Phys. 11 (2014) 064.
[59] P. Romatschke, Relativistic fluid dynamics far from local equilibrium, Phys. Rev. Lett. **120**, 012301 (2018).
[60] M. Baggioli, L. Li, and H. T. Sun, Shear flows in far-from-equilibrium strongly coupled fluids, Phys. Rev. Lett. **129**, 011602 (2022).
[61] C. Cartwright, M. Kaminski, and M. Knipfer, Hydrodynamic attractors for the speed of sound in holographic Bjorken flow, Phys. Rev. D **107**, 106016 (2023).
[62] L. V. Delacrétaz, B. Goutéraux, and V. Ziogas, Damping of pseudo-Goldstone fields, Phys. Rev. Lett. **128**, 141601 (2022).
[63] A. Jain and P. Kovtun, Schwinger-Keldysh effective field theory for stable and causal relativistic hydrodynamics, arXiv:2309.00511.
[64] N. Mullins, M. Hippert, L. Gavassino, and J. Noronha, Relativistic hydrodynamic fluctuations from an effective action: Causality, stability, and the information current, Phys. Rev. D **108**, 116019 (2023).
[65] N. Mullins, M. Hippert, and J. Noronha, Stochastic fluctuations in relativistic fluids: causality, stability, and the information current, Phys. Rev. D **108**, 076013 (2023).
[66] Y. Nambu, Dispersion relations for form factors, Nuovo Cimento **9**, 610 (1958).
[67] R. Karplus, C. M. Sommerfield, and E. H. Wichmann, Spectral representations in perturbation theory. 1. Vertex function, Phys. Rev. **111**, 1187 (1958).
[68] A. Windisch, M. Q. Huber, and R. Alkofer, How to determine the branch points of correlation functions in Euclidean space, Acta Phys. Pol. B Proc. Suppl. **6**, 887 (2013).
[69] M. Q. Huber, W. Kern, and R. Alkofer, On the analytic structure of three-point functions from contour deformations, Phys. Rev. D **107**, 074026 (2023).